

# Ab Initio and Semiempirical Conformation Potentials for Phospholipid Head Groups

Johan Landin and Irmin Pascher

Department of Medical Biochemistry and MEDNET Laboratory, Göteborg University,  
Medicinaregatan 9, S-413 90 Göteborg, Sweden

Dieter Cremer\*

Department of Theoretical Chemistry, Göteborg University, Kemigården 3, S-412 96 Göteborg, Sweden

Received: September 14, 1994; In Final Form: January 3, 1995<sup>⊗</sup>

The conformational potential of the dimethyl phosphate (DMP) anion and the 2-ammonioethanol (AME) cation, which are substructures of the phosphoethanolamine head group of phospholipids, has been investigated at the Hartree–Fock (HF) level using the 3-21G, 3-21G(\*), 6-31G\*, and 6-31+G\* basis set. For this purpose, both the DMP anion and the AME cation were considered as geminal double rotors with the two rotor groups OCH<sub>3</sub> in the case of DMP and OH and CH<sub>2</sub>NH<sub>3</sub><sup>+</sup> in the case of AME. Extensive scans (17 points including eight stationary points for DMP and 30 points including seven stationary points for AME) of the conformational energy surface were carried out by complete geometry optimizations at the HF/3-21G and HF/3-21G(\*) levels, respectively, and subsequent single point calculations with larger basis sets. The most stable DMP form has the two OCH<sub>3</sub> groups in syn-clinal (+sc) positions (both dihedral angles  $\alpha_2$  and  $\alpha_3 = 75.3^\circ$ ) while the AME cation prefers an anti-periplanar (ap) ( $\alpha_4 = 173.3^\circ$ ), syn-clinal (+sc) ( $\alpha_5 = 48.5^\circ$ ) conformation with regard to the OH and CH<sub>2</sub>NH<sub>3</sub><sup>+</sup> groups. The DMP anion is a rather flexible rotor that can undergo various flip-flop rotations (barriers 1 and 6 kcal/mol) that indicate strong coupling between the rotor groups. The AME cation, on the other hand, is conformationally not flexible, which has to do with the fact that the two rotor groups OH and CH<sub>2</sub>NH<sub>3</sub><sup>+</sup> are electronically very different. The preferred rotational processes of the AME cation involve inwardly or outwardly directed rotations at the CC bond (barriers of 5.1 and 9.3 kcal/mol) with the OH group kept essentially in an ap position. Calculations reveal that semiempirical methods such as PM3 are not able to describe the conformational tendencies of either DMP anion or AME cation correctly.

## 1. Introduction

Phospholipids are important components of biological membranes, and in order to understand the specific roles of different phospholipids for membrane structure and function, a detailed structural knowledge of the membrane constituents is necessary, particularly concerning the conformation and interactions of the polar lipid head groups at the membrane surface. During recent years structural information with atomic resolution of a great number of complex membrane lipids has become available from X-ray single crystal analysis.<sup>1</sup> Especially regarding zwitterionic phosphoethanolamine lipids, the structures of a dozen of model compounds with varying numbers of *N*-methyl groups have been solved, comprising polar head groups and single chain and double chain lipids. When comparing these structures, it is surprising that in all of them the zwitterionic phosphoethanolammonium groups, despite of differences in the degree of *N*-methylation and hydration and variations in head group packing and intermolecular interactions, adopt very similar preferred conformations. This suggests that the conformation of the phosphoethanolamine group is governed by strong intramolecular interactions and that the varying crystal environment does not significantly affect the conformational preference of the phosphoammonium zwitterion. The aim of the present work is to understand the energetics which determine these preferred conformational features and to test computational methods for predicting phospholipid head group conformations when no experimental data are available.

There have been many calculations on phospholipid head groups, but most of them were done with methods which are

now considered to be outdated because of their lack of precision. Pullman and co-workers pioneered the work with Hartree–Fock (HF)/STO-3G and PCILO (perturbative configuration interaction using localized orbitals) methods.<sup>2–4</sup> They found that in the gas phase the most stable conformation of the phosphoethanolamine head group is a ring-like structure stabilized by a hydrogen bond between the ammonium and the phosphate group. Further calculations by Pullman and co-workers suggest that if the head group is hydrated it adopts the more extended form observed in crystals. Calculations on a phosphoethanolamine head groups in a planar, two-dimensional lattices were done by Frischleder and co-workers.<sup>5,6</sup> They used both PCILO and PCILOCC (perturbative configuration interaction using localized orbitals for crystal calculations) and found that the extended form found in crystals was stabilized by intermolecular interactions, especially hydrogen bonds. In absence of intermolecular forces, other conformations were lower in energy. The existence of an intermolecular coupling between the head groups was also found by Kreissler and co-workers, who analyzed a system composed of seven 1,2-dipalmitoyl-*sn*-glycero-3-phosphoethanolamine molecules interacting with each other.<sup>7</sup> With an empirical force field method, coupling was predicted between the conformations of two neighboring molecules, affecting the head groups as well as the glycerol backbone regions.

During recent years ab initio calculations on substructures of the phosphoethanolamine head group have been presented by several groups. Hadzi and co-workers presented frequency calculations on the dimethyl phosphate (DMP) anion and several of its salts. They compared their theoretical results with experimental data, focusing the discussion on the behavior and

<sup>⊗</sup> Abstract published in *Advance ACS Abstracts*, March 1, 1995.

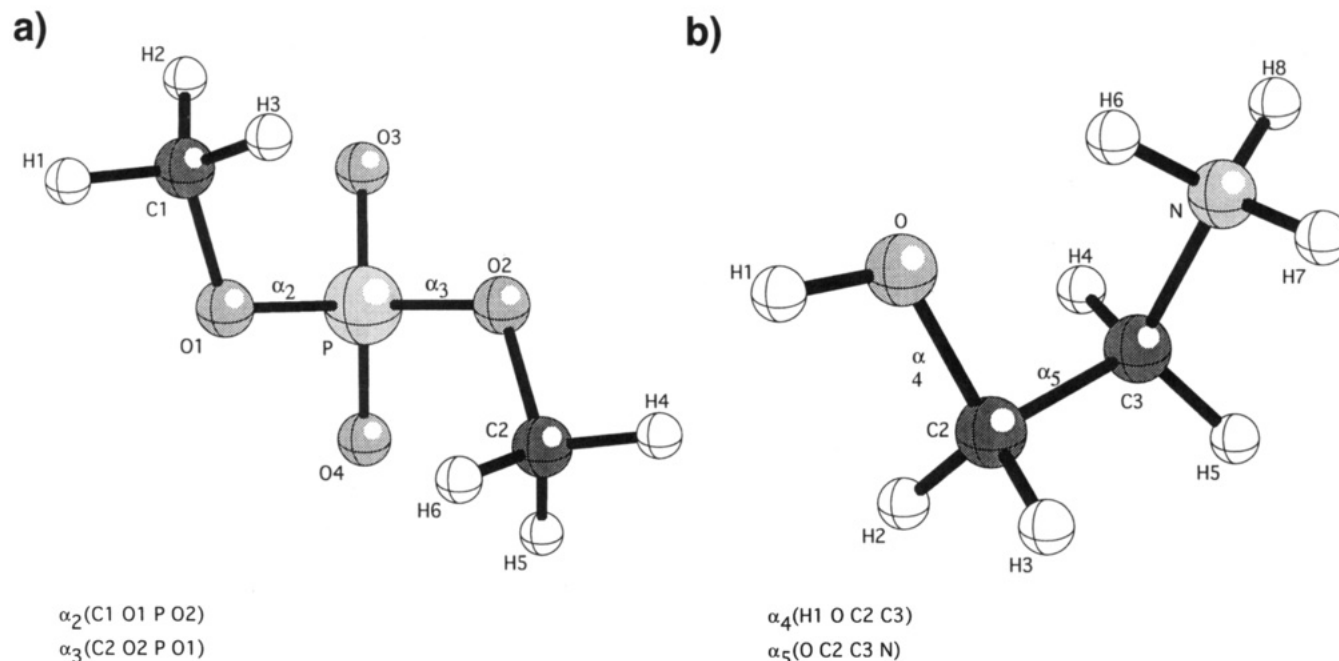


**Figure 1.** Labeling of atoms and notation of geometry parameters of (a) the dimethyl phosphate (DMP) anion and (b) the 2-ammonioethanol (AME) cation.

vibrational character of the  $\text{PO}_2^-$  frequencies.<sup>8</sup> High-level ab initio calculations have been presented by Liang and co-workers. They discuss in detail the conformational space of two phospholipid model compounds, namely the dimethyl phosphate (DMP) anion and the methyl propyl phosphate (MPP) anion. However, their discussion is based on just a few calculations and, accordingly, a potential energy surface is not presented in their paper.<sup>9</sup>

In this paper, we will make a detailed investigation of the in vacuo conformation potentials for two substructures of the phosphoethanolamine head group, namely the dimethyl phosphate (DMP) anion and the 2-ammonioethanol (AME) cation with both ab initio and semiempirical methods. Corresponding calculations on the entire phospholipid head group, as well as calculations including environmental effects, will be presented in a following paper. With this stepwise approach we want to accomplish two objectives. First, we want to find the right method for a quantum chemical description of the phospholipid head group. Second, we want to gain a deeper understanding of the conformational behavior of phospholipids, in particular of the arrangement and properties of the head groups at the membrane surface.

## 2. Computational Methods

All semiempirical calculations were carried out with the PM3<sup>10,11</sup> parametrization as implemented in the MOPAC program version 6.<sup>12</sup> Ab initio calculations were performed at the Hartree-Fock (HF) level using three basis sets of DZ+P quality, namely the 3-21G(\*),<sup>13-15</sup> the 6-31G\*,<sup>16-19</sup> and the 6-31+G\*<sup>16-19</sup> basis sets of Pople and co-workers. The 3-21G(\*) basis, which contains a set of six d-functions for second-row atoms, was employed for geometry optimizations while the two other basis sets were used for single point calculations at HF/3-21G(\*) geometries. These levels of theory are denoted by HF/6-31G\*\*/HF/3-21G(\*) and HF/6-31+G\*\*/HF/3-21G(\*). It is well-known that the diffuse charge distribution of an anion such as the DMP anion can only be correctly described by including diffuse functions into the basis set.<sup>20,21</sup> Accordingly, the 6-31+G\* basis, which contains both a set of diffuse sp

functions and d-type polarization functions for all heavy atoms, does provide the best description of DMP. However, it is also known that diffuse functions are not so important in order to get a reliable geometry of an anion.<sup>22</sup> Therefore, one can expect that the most reliable description of the DMP anion is obtained at the HF/6-31+G\*\*/HF/3-21G(\*) level of theory.

For the AME cation, we have used the 3-21G basis<sup>13-15</sup> (equivalent with the 3-21G(\*) basis for the phosphorus compound DMP) for geometry optimizations. It turned out that the HF/3-21G conformational surface constrains the AME cation to a rather limited area close to the global minimum since most other conformational regions are of relatively high energy ( $\Delta E > 20$  kcal/mol). This was confirmed by test calculations at the HF/6-31G\*\*/HF/3-21G level of theory. Accordingly, we have refrained from recalculating the whole conformational surface at HF/6-31G\*\*/HF/3-21G.

For the global minimum of DMP and AME, we repeated geometry optimizations at the HF and second-order Møller-Plesset (MP2) perturbation theory<sup>23</sup> levels using Pople's 6-31G\* basis.<sup>17</sup> In this way, we checked both the influence of employing a full set of polarization functions on all heavy atoms and that of electron pair correlation effects on calculated geometries. In the case of DMP, these calculations were extended to the conformation located at the local minimum closest in energy in order to check the possibility of stability reordering because of basis set correlation effects. In the case of AME, this test is not necessary in view of the fact that the lowest energy difference between global and local minima is larger than 7 kcal/mol.

Atom labeling and torsion angle notations for DMP anion and AME cation are defined in Figure 1. The notations for torsional angles follow the convention for phospholipids given by Sundaralingam,<sup>24</sup> where a dihedral angle  $\alpha$  of  $0^\circ$  corresponds to a syn-periplanar (sp) form. By this all other possible conformers such as the syn-clinal ( $\alpha = 60^\circ$ , +sc), anti-clinal ( $\alpha = 120^\circ$ , +ac), and anti-periplanar ( $\alpha = 180^\circ$ , ap) forms are defined. The numbering of dihedral angles for both DMP and AME corresponds to the notations used in conformational descriptions of complete phospholipids.<sup>1</sup>

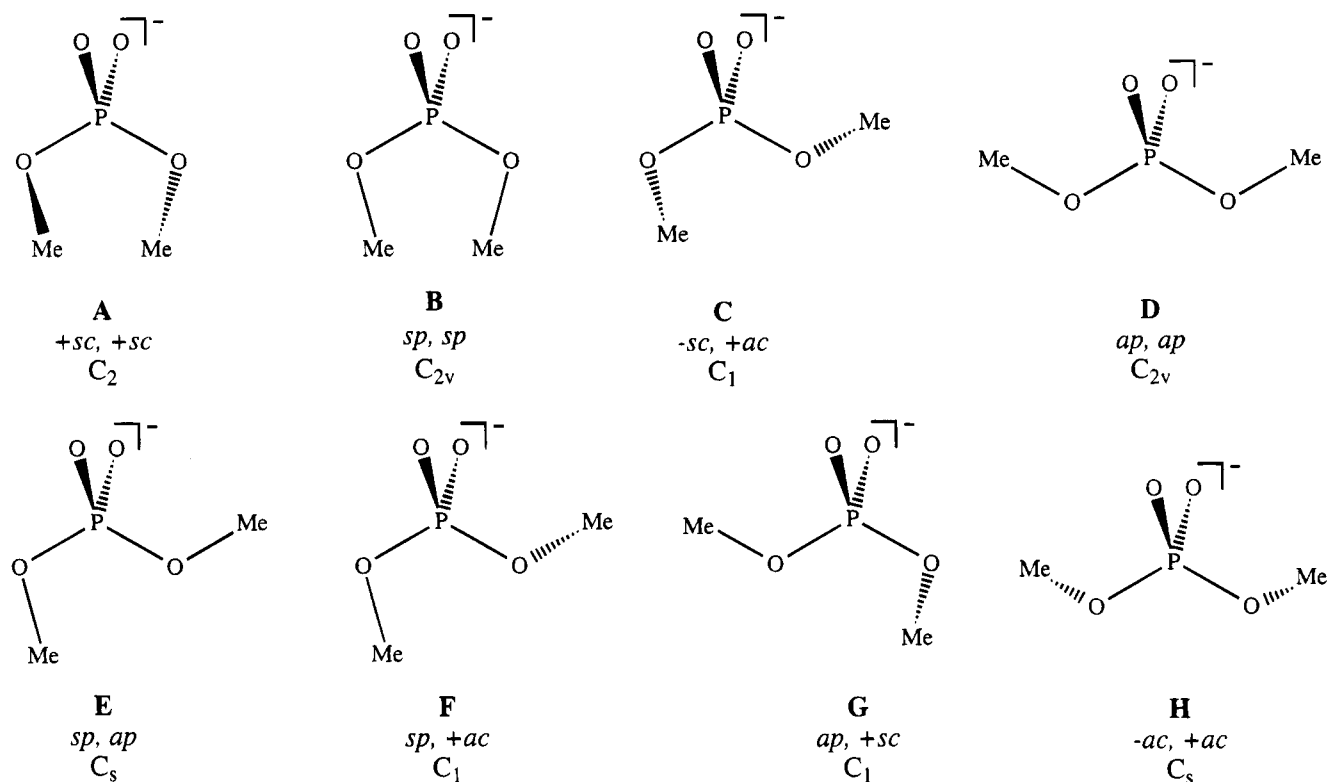


**Figure 2.** Conformers of the dimethyl phosphate (DMP) anion that are located at the stationary points of the ab initio conformational energy surface. The abbreviations +sc,+sc, sp,sp, etc., denote sign and range of the dihedral angles  $\alpha_2$  and  $\alpha_3$ : sp, syn-periplanar; ap, anti-periplanar; sc, syn-clinal; ac, anti-clinal.

The conformational space of DMP is spanned by four rotational angles, two of which, namely  $\alpha_2$  and  $\alpha_3$  (see Figure 1a), are systematically varied to explore the conformational subspace spanned by  $\alpha_2$  and  $\alpha_3$ . Thus, DMP is treated as a geminal double rotor, for which all geometrical parameters were optimized for each conformer considered. Apart from this, all stationary points in the  $\alpha_2, \alpha_3$  space were determined by optimization of all geometrical parameters. Previous ab initio investigations of geminal double rotors<sup>25</sup> such as the DMP anion have shown that their conformational potential can be characterized by a relatively small number of stationary points, which are occupied by typical conformers of a geminal double rotor. For the PM3  $\alpha_2, \alpha_3$  conformational surface of the DMP anion, we have identified seven stationary points labeled by capital letters A–G (Figure 2), which are the location of +sc,+sc (A), sp,sp (B), -sc,+sc (C), ap,ap (D), sp,ap (E), sp,+sc (F), and ap,+sc (G) conformers. At the ab initio level, the position of some of the stationary points changed strongly and, in addition, new stationary points (H, I, etc.) appeared, which we have investigated in each case by full geometry optimizations and subsequent calculations of the eigenvalues of the Hessian matrix. In this way, a total of 17 unique surface points were calculated. For  $C_1$ -symmetrical DMP anion forms, this led to geometry optimizations of 33 variables.

The conformational space of the AME cation is spanned by three dihedral angles of which angles  $\alpha_4$  and  $\alpha_5$  defined in Figure 1b were varied in the same way as  $\alpha_2$  and  $\alpha_3$  for the DMP anion, i.e. the AME cation was also treated as a geminal double rotor. Since the two rotating groups (OH and  $\text{CH}_2\text{NH}_3^+$ ) are different, the  $\alpha_4, \alpha_5$  conformational surface of AME has lower symmetry ( $C_2$ ) compared to that of the  $\alpha_2, \alpha_3$  surface of DMP ( $C_{2v}$ ). As a consequence, a total of 30 surface points plus the derivative information of six selected stationary points was necessary to get a reasonable description of the total  $\alpha_4, \alpha_5$  surface.

Analytical forms of the DMP and AME conformational energy surfaces were obtained by following a procedure developed by Cremer.<sup>25</sup> First, calculated surface points were fitted to a Fourier expansions. Then, Fourier terms with small coefficients were eliminated where the quality of the surface fit was tested by standard deviation  $\sigma$  and correlation coefficient  $r^2$ . Once the best Fourier expansion was calculated, all stationary points of the conformational energy surface were determined from the Fourier expansion and compared with directly calculated stationary points. For both DMP and AME, additional stationary points were found in this way (see above), which in turn were confirmed by appropriate ab initio calculations and used to improve the surface fit. However, in the case of some high-lying stationary points of the AME surface ( $\Delta E > 15$  kcal/mol), we refrained from an explicit confirmation by ab initio calculations.

After determining all stationary points and having obtained the best surface fit, each Fourier term was identified with a specific electronic effect (dipole–dipole interactions, anomeric delocalization, bond staggering, and couplings between these effects) and their influence on specific features of the conformational energy surface analyzed. In this way, a detailed account of the conformational features of the DMP anion and the AME cation and their dependence on special electronic effects was possible.

### 3. Results and Discussion

In Table 1, PM3 and ab initio conformational energies are listed for the most important stationary points of the DMP anion surface while calculated geometry parameters of the corresponding DMP anion conformers are given in Table 2. The geometry of the global minimum conformation A is presented in Figure 3. Contourline drawings and perspective three-dimensional drawings of the calculated DMP conformational

**TABLE 1: Calculated Energies for Selected Conformations of the Dimethyl Phosphate (DMP) Anion<sup>a</sup>**

conf <sup>b</sup>	sym	PM3			sym	HF/3-21G(*)			HF/6-31G*//3-21G(*)	HF/6-31+G*//3-21G(*)
		$\alpha_2$	$\alpha_3$	$\Delta E$		$\alpha_2$	$\alpha_3$	$\Delta E$	$\Delta E$	$\Delta E$
A <sub>1</sub>	C <sub>2</sub>	65.9	65.9	0.0	C <sub>2</sub>	74.9	74.9	0.0	0.0	0.0
B	C <sub>2v</sub>	0.0	0.0	6.1	C <sub>2v</sub>	0.0	0.0	20.0	20.9	20.5
C <sub>1</sub>	C <sub>s</sub>	-80.3	80.3	-0.4	C <sub>1</sub>	-65.0	146.3	0.7	1.5	1.6
D <sub>1</sub>	C <sub>2v</sub>	180.0	180.0	2.6	C <sub>2v</sub>	180.0	180.0	3.2	2.6	2.5
E <sub>1</sub>	C <sub>s</sub>	0.0	180.0	2.7	C <sub>s</sub>	0.0	180.0	3.6	5.3	5.6
F <sub>1</sub>	C <sub>1</sub>	-5.6	80.3	1.4	C <sub>1</sub>	1.3	138.6	3.0	6.0	6.5
G <sub>1</sub>	C <sub>1</sub>	180.0	73.7	1.3	C <sub>1</sub>	175.9	68.9	1.2	1.0	0.9
H <sub>1</sub>					C <sub>s</sub>	-97.0	97.0	1.7	3.1	3.2
		HF/6-31G*				MP2/6-31G*				
A <sub>1</sub>	C <sub>2</sub>	75.1	75.1	0.0	C <sub>2</sub>	71.4	71.4	0.0		
C <sub>1</sub>	C <sub>1</sub>	-73.8	170.6	1.2	C <sub>1</sub>	-71.5	163.6	1.4		

<sup>a</sup> Dihedral angles  $\alpha_i$  in degrees, relative energies in kcal/mol. All energy data relative to the energy of conformer A. Heat of formation of A: -275.2 kcal/mol (PM3); absolute energies of A: -715.84778 au (HF/3-21G\*), -719.51785 au (HF/6-31G\*//HF/3-21G\*), -719.54071 au (HF/6-31+G\*//HF/3-21G\*), -719.52087 au (HF/6-31G\*), and -720.64766 au (MP2/6-31G\*). <sup>b</sup> For the notation of conformers, see Figure 2.

**TABLE 2: Calculated Geometry Parameters for Selected Conformers of the Dimethyl Phosphate (DMP) Anion**

conformer <sup>a</sup>	A <sub>1</sub>	B	C <sub>1</sub>	D <sub>1</sub>	E <sub>1</sub>	F <sub>1</sub>	G <sub>1</sub>	H <sub>1</sub>
A. PM3								
P-O3	1.495	1.488	1.498	1.497	1.493	1.490	1.498	
P-O4	1.495	1.488	1.491	1.497	1.493	1.494	1.494	
P-O1	1.767	1.775	1.768	1.767	1.763	1.772	1.758	
P-O2	1.767	1.775	1.768	1.767	1.778	1.770	1.776	
O1-C1	1.372	1.363	1.372	1.373	1.370	1.368	1.374	
O2-C2	1.372	1.363	1.372	1.373	1.371	1.373	1.371	
O3-P-O4	126.6	128.2	126.8	124.7	126.0	127.1	125.7	
O1-P-O2	99.4	110.0	99.1	93.8	99.4	102.4	96.3	
P-O1-C1	119.7	129.0	119.7	115.5	122.7	123.9	119.1	
P-O2-C2	119.7	129.0	119.7	115.5	116.7	120.1	116.4	
$\alpha_2$ (C1-O1-P-O2)	65.9	0.0	-80.3	180.0	0.0	-5.6	180.0	
$\alpha_3$ (C2-O2-P-O1)	65.9	0.0	80.3	180.0	180.0	80.3	73.7	
B. HF/3-21G(*)								
P-O3	1.473	1.472	1.481	1.478	1.475	1.473	1.478	1.484
P-O4	1.473	1.472	1.470	1.478	1.475	1.479	1.472	1.468
P-O1	1.634	1.636	1.640	1.627	1.623	1.628	1.621	1.632
P-O2	1.634	1.636	1.623	1.627	1.643	1.642	1.640	1.632
O1-C1	1.435	1.407	1.434	1.436	1.428	1.426	1.436	1.432
O2-C2	1.435	1.407	1.434	1.436	1.434	1.433	1.434	1.432
O3-P-O4	124.6	123.2	122.9	120.5	121.6	122.2	122.5	123.5
O1-P-O2	98.3	103.3	97.0	95.7	96.3	97.0	96.6	100.5
P-O1-C1	118.2	138.7	119.1	116.1	124.3	124.2	118.5	121.3
P-O2-C2	118.2	138.7	118.4	116.1	116.1	119.8	116.5	121.3
$\alpha_2$ (C1-O1-P-O2)	74.9	0.0	-65.0	180.0	0.0	1.3	175.9	-97.0
$\alpha_3$ (C2-O2-P-O1)	74.9	0.0	146.3	180.0	180.0	138.6	68.9	97.0

<sup>a</sup> For the notation of the conformers, see Figure 2.

surfaces are shown in Figures 4a and 5a (PM3), 4b and 5b (HF/3-21G\*), and 4c and 5c (HF/6-31+G\*//HF/3-21G\*). All graphical representations are based on a least squares fit of calculated surface points to a Fourier expansion, the analytical representation of which is given in Table 3. Total atomic charges calculated with different methods for the global minimum of DMP are listed in Table 4.

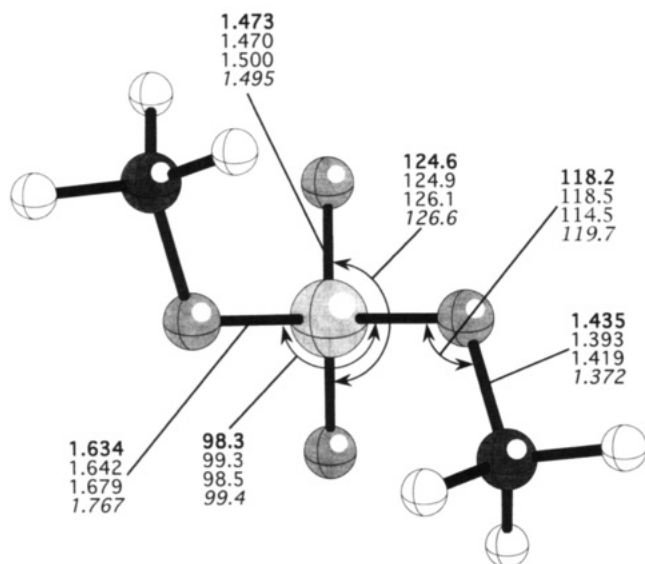
The corresponding data for the AME cation can be found in Tables 5 (calculated conformational energies), 6 (calculated geometries), 7 (Fourier analysis of the  $\alpha_4, \alpha_5$  conformational surface), and 8 (calculated charges). Figure 6 gives PM3 and ab initio geometries of the global minimum conformation of the AME cation while the calculated  $\alpha_4, \alpha_5$  surfaces are shown in Figures 7 and 8 (a, PM3; b, HF/3-21G). For  $\alpha_4$  and  $\alpha_5$ , the same range of values was chosen to compare the AME conformational surface with the DMP surface. However, it turned out that this did not lead to a satisfying view of the region of the global minimum and, therefore, in Figures 7c and 8c, the HF/3-21G surface is given once more for a different range of  $\alpha_4$  values.

### 3.1. Conformational Energy Surface of the DMP Anion.

The conformational energy surface of DMP possesses C<sub>2v</sub>

symmetry,<sup>26</sup> which is confirmed at all levels of theory used as can be seen from Figure 4. The conformational surfaces obtained at the HF/3-21G(\*) and PM3 levels of theory show similar features (see Figures 4 and 5), but they differ with regard to important details. We will show in the following that the HF/3-21G(\*) surface is more reliable than the PM3 surface. Therefore, we will preferentially discuss the former while pointing out just some differences with regard to the later.

Both methods predict a global maximum B of relatively high energy (PM3, 6; HF/3-21G(\*), 20 kcal/mol; Table 1) at the position  $\alpha_2 = \alpha_3 = 0^\circ$ , which is occupied by the sp,sp form (Figure 2). The maximum is surrounded by four regions of relatively low energy, which are the locations of four (PM3) or six (ab initio) energy minima that correspond to the +sc,+sc (global minimum A) and -sc,+sc (-sc,+ac) conformations (local minimum C) of the DMP anion. Energy valleys indicated by dashed lines in Figure 4 connect the minima thus forming a path of minimum energy that surrounds the central maximum B. Highest points of the minimum energy path are four equivalent first-order transition states F that represent the energy barriers for rotational interconversion between +sc,+sc and -sc,+sc (-sc,+ac) conformations.



$$\alpha_2 = \alpha_3 = 74.9 \text{ HF/3-21G(*)}$$

$$\alpha_2 = \alpha_3 = 75.1 \text{ HF/6-31G*}$$

$$\alpha_2 = \alpha_3 = 71.4 \text{ MP2/6-31G*}$$

$$\alpha_2 = \alpha_3 = 65.9 \text{ PM3}$$

**Figure 3.** Minimum energy conformation of the dimethyl phosphate (DMP) anion. HF/3-21G(\*) values for heavy atom bond lengths and angles are given in bold print (HF/6-31G\*, normal, MP2/6-31G\*, normal, PM3, italics).

While HF/3-21G(\*) predicts the +sc,+sc form at A to be most stable, PM3 gives the -sc,+sc conformation at C to be 0.4 kcal/mol lower in energy than conformation A. At the ab initio level, the differences between these two conformations are 0.7 (HF/3-21G\*), 1.5 (HF/6-31G\*/HF/3-21G-\*), 1.2 (HF/6-31G\*), 1.6 (HF/6-31+G\*/HF/3-21G-\*), and 1.4 kcal/mol (MP2/6-31G\*), respectively, in favor of A. Conformation A possesses  $C_2$  symmetry at all levels of theory, i.e. the dihedral angles  $\alpha_2$  and  $\alpha_3$  adopt the same values for this conformation (HF/3-21G(\*),  $\alpha_2 = \alpha_3 = 74.9^\circ$ ; HF/6-31G\*,  $75.1^\circ$ ; MP2/6-31G\*,  $71.4^\circ$ ; PM3,  $65.9^\circ$ ; Table 1).

The preference of  $\alpha_2, \alpha_3$  for +sc,+sc or -sc,-sc, corresponding to conformers  $A_1$  and  $A_2$ , is well-documented by experimental results. Of 15 reported crystal structures of phosphoethanolamine compounds,<sup>1,27</sup> 14 show the  $A_1/A_2$  conformation, usually as coexisting mirror images. Experimentally, the  $\alpha_2$  values were observed to range from  $53^\circ$  to  $86^\circ$  (average  $66.5^\circ$ ) and the  $\alpha_3$  values from  $45^\circ$  to  $81^\circ$  (average  $62.8^\circ$ ). Only one example of the ap,+sc ( $177^\circ, 67^\circ$ ) conformer, corresponding to conformation C obtained at the HF/6-31+G\* level of theory, has been observed.<sup>28</sup> A broader search on all types of phosphodiester in the Cambridge structural database<sup>29</sup> confirms the predominance of the +sc,+sc or -sc,-sc conformer. Of a total of 131 phosphodiester, 109 (=83%) exist in the +sc,+sc (or -sc,-sc) conformation A while 17 (=13%) and five (=4%) were found to adopt the ap,+sc (+sc,ap) and +ac,+sc (+sc,+ac) conformation C, respectively.

The predominance of the A conformer is in excellent agreement with our ab initio calculations and also the occurrence of ap,+sc (+sc,ap) and +ac,+sc (+sc,+ac) conformers C (Table 1). For the global minimum energy conformation predicted by PM3, the -sc,+sc conformer C (Table 1 and Figure 4a), we have so far not found any experimental evidence.

At the PM3 level,  $\alpha_2$  is calculated to be  $-\alpha_3$  at C thus indicating  $C_s$  symmetry for the -sc,+sc form. However, HF/3-21G(\*) leads to a  $C_1$ -symmetrical -sc,+ac conformation at

C with  $\alpha_2 = -65^\circ$  and  $\alpha_3 = 146^\circ$ . Accordingly, there exists a second C conformation at  $\alpha_2 = -146^\circ$  and  $\alpha_3 = 65^\circ$  (-ac,+sc), thus leading to a total of four C conformations rather than two found at the PM3 level of theory. At higher levels of theory, the two C minima move even further apart to -sc,ap and ap,+sc positions (HF/6-31G\*,  $\alpha_2 = \alpha_3 = -73.8^\circ, 170.6^\circ/-170.6^\circ, 73.8^\circ$ ; HF/6-31+G\* (Fourier fit),  $-70^\circ, 175^\circ/-175^\circ, 70^\circ$ ; MP2/6-31G\*,  $-71.5^\circ, 163.6^\circ/-163.6^\circ, 71.5^\circ$ ; Table 1). Each pair of C conformations is connected by a low-energy path via the saddle point H (see Figures 4b and 5b). Form H has  $C_s$  symmetry and is located at  $\alpha_2 = -97^\circ$  and  $\alpha_3 = 97^\circ$ , i.e. it resembles the C forms found at the PM3 level (Table 1). Transition state H is also found at the HF/6-31G\* and the HF/6-31+G\* surfaces (Table 1, Figures 4c and 5c). Its relative energies are 1.7 (HF/3-21G(\*)), 3.1 (HF/6-31G\*), and 3.2 kcal/mol (HF/6-31+G\*, Table 1), which means that the rotational barrier separating the two C forms corresponds to just 1 (HF/3-21G(\*)), 1.6 (HF/6-31G\*), and 1.6 kcal/mol (HF/6-31+G\*), respectively. The latter energy differences may be somewhat exaggerated because of imposing HF/3-21G(\*) geometries for forms C and H, but in any case, there is a shallow minimum area between  $\alpha_2 = -60^\circ$  ( $150^\circ$ ),  $\alpha_3 = 150^\circ$  ( $-60^\circ$ ) and  $\alpha_2 = -150^\circ$  ( $60^\circ$ ),  $\alpha_3 = 60^\circ$  ( $-150^\circ$ ).

The highest energy barrier that the molecule has to surmount when following the minimum energy path surrounding energy maximum B is given by the relative energy of transition state F, which is 3 kcal/mol at the HF/3-21G(\*) level but about 6 kcal/mol at the two higher levels of theory (Table 1). Again, PM3 predicts a much lower relative energy (1.4 kcal/mol, Table 1). The conformer sitting at F has one OCH<sub>3</sub> group in a sp position while the other group is in a  $\pm$ sc (PM3,  $\alpha_3 = 80.3^\circ$ ; Table 1),  $\pm$ ac position (HF/3-21G(\*),  $\alpha_3 = 138.6^\circ$ ; Table 1) or ap position (HF/6-31+G\*,  $\alpha_3 = 180^\circ$ ; Figure 4c).

For PM3 and HF/3-21G(\*), there exist local maxima in the ap,ap range (D, Figure 4a,b) and the sp,ap/ap,sp range (E). At the higher ab initio levels, D moves toward the ac,ac range while maxima E merges with the saddle point F. The maxima have similar relative energies at the PM3 level (2.6, 2.7 kcal/mol, Table 1) and HF/3-21G(\*) level (3.2, 3.6 kcal/mol), but range from 3.1 to 5.6 kcal/mol at the 6-31+G\* level (Figure 4c and Table 1), taking into account that D is shifted toward the ac,ac range. The minimum energy paths encircling maxima D and E pass through the saddle points G and H (path encircling D) as well as F and G (path encircling E). The PM3 transition state  $G_1$  is located at  $\alpha_2 = 180^\circ$  and  $\alpha_3 = 74^\circ$  while at the HF/3-21G(\*) and HF/6-31+G\* level transition state  $G_1$  is shifted to somewhat smaller  $\alpha_2, \alpha_3$  values ( $175.9^\circ, 68.9^\circ$  and  $135^\circ, 75^\circ$ , respectively; Table 1 and Figure 4c). Transition states G and H represent very low rotational barriers (1–2 kcal/mol, Table 1), hindering a rotation from the global minimum A to a local minimum C and between pairs of local minima C (compare with Figures 4 and 5).

**Preferred Conformational Processes of DMP.** If DMP follows the minimum energy path  $A_1-F_1-C-F_2-A_2-F_3-C-F_4-A_1$  (path 1) surrounding the maximum B, the +sc,+sc form  $A_1$  is inverted into the -sc,-sc form  $A_2$  and back into itself. Such an inversion could be thought of as occurring in the same way as the ring inversion of a five-membered ring, namely passing through a planar ring form which would correspond to the sp,sp form B of DMP. However, this would involve a synchronous disrotatory movement of both methoxy groups that would lead to considerable steric repulsion and a high-energy barrier at form B. Both geminal double rotors such as DMP and five-membered rings avoid inversion processes.<sup>25,30–32</sup> Instead DMP prefers a conformational process that implies a

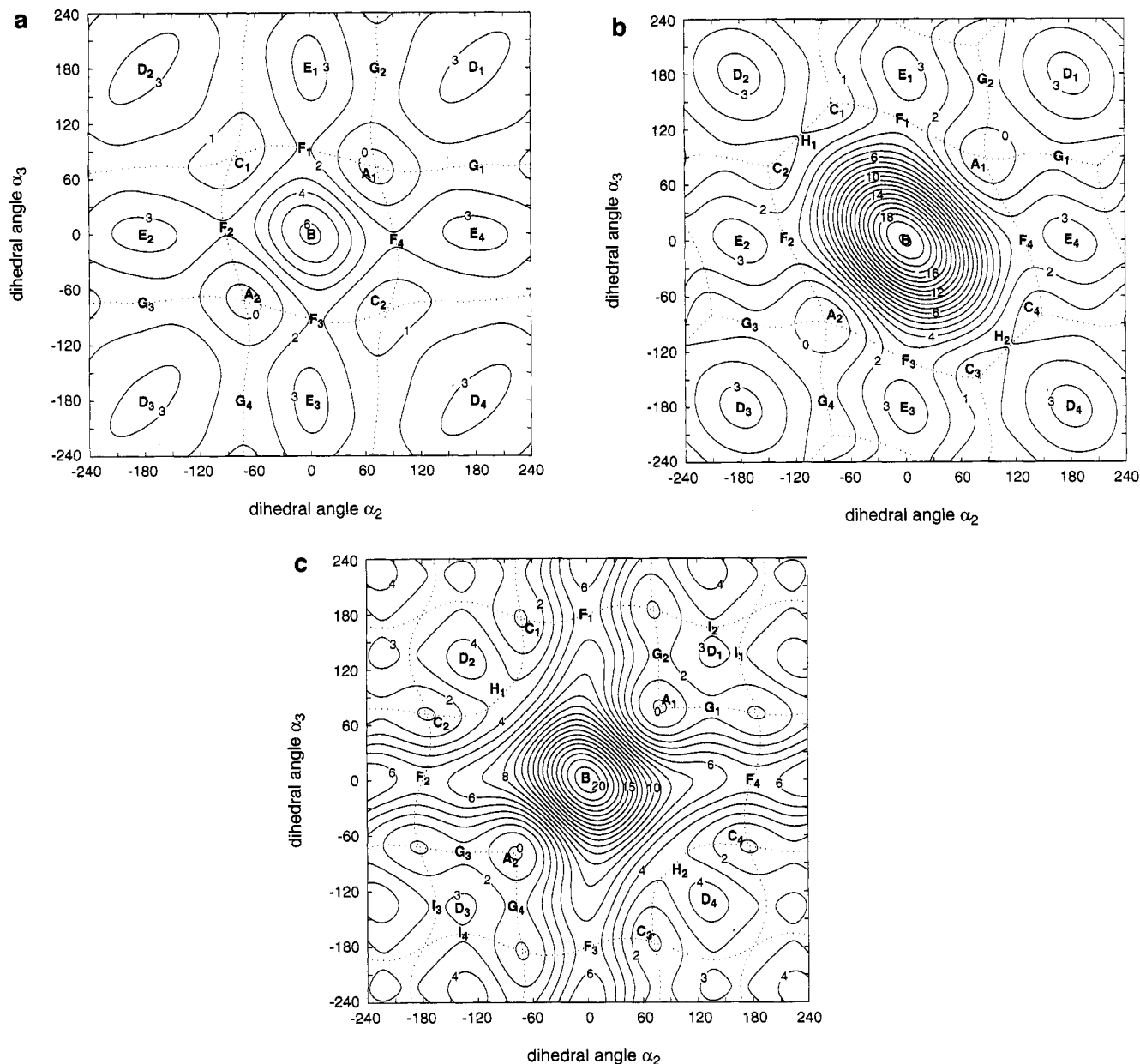


**Figure 4.** Contour line diagram of the  $\alpha_2, \alpha_3$ -conformational energy surface of the dimethyl phosphate (DMP) anion. (a) PM3 surface, (b) HF/3-21G(\*) surface, and (c) HF/6-31+G\*\*/HF/3-21G(\*) surface. Contour levels in kcal/mol are given in small print. Stationary points are indicated by capital letters in bold print according to the notation given in Figure 2. Equivalent stationary points are numbered according to their appearance in the first, second, etc.,  $\alpha_2, \alpha_3$  quadrant of the conformational space. Minimum energy paths connecting global and local energy minima as well as intermediate saddle points are given by dashed lines. The range of  $\alpha$ -values has been chosen to be  $\pm 240^\circ$  rather than  $\pm 180^\circ$  to show the periodicity of the potential and to facilitate investigation of the area around the local maxima D. Note that at the HF/6-31+G\*\*/HF/3-21G(\*) level the local maxima E disappear in the sp,ap region while in the ap,ap region new saddle points (I) appear.

stepwise rotation of the methoxy groups: First, one OCH<sub>3</sub> group rotates inwardly into and through the plane defined by atoms P, O1, and O2 (Figure 1). This corresponds to a movement along the dashed line from the global minimum A up the valley to the saddle point F (see Figure 4) and, then, down the next valley to the local minimum C. When C is reached (PM3 surface; point H, ab initio surfaces, see below), both OCH<sub>3</sub> groups are in positions that define the envelope conformation of a five-membered ring (see Scheme 1).

In the next step of the conformational process indicated by path 1, the second OCH<sub>3</sub> group rotates inwardly through the P–O1–O2 plane until the –sc, –sc form A<sub>2</sub> is reached, again passing through a saddle point F. Since both A forms possess C<sub>2</sub> symmetry with the two OCH<sub>3</sub> groups at different sides of the P–O1–O2 plane, they correspond to twist and inverted twist conformation of a five-membered ring (see Scheme 1). Con-

tinuation along path 1 leads to the +sc, –sc C form (PM3 surface; point H, ab initio surfaces, see below) and, finally, back to the starting +sc, +sc form A<sub>1</sub>.

The conformational process defined by path 1 has been coined *flip-flop rotation of a geminal double rotor*, and it has been shown (see also Scheme 1) that it corresponds to the *pseudorotation of a nonplanar five-membered ring*.<sup>25,30–32</sup> While PM3 predicts a flip-flop process parallel to a pseudorotation of five-membered rings (see Figure 4a), ab initio theory suggests a somewhat more complicated rotational process that deviates from the pseudorotation mode of five-membered rings. Any time one OCH<sub>3</sub> group rotates through the plane P–O1–O2, the other OCH<sub>3</sub> group rotates into an ac conformation ( $\alpha = 140\text{--}150^\circ$ , Table 1, see also Figure 4b and Scheme 1) in order to arrange the lone pairs of its O atom for more effective interactions with the H atoms of the neighboring methyl group



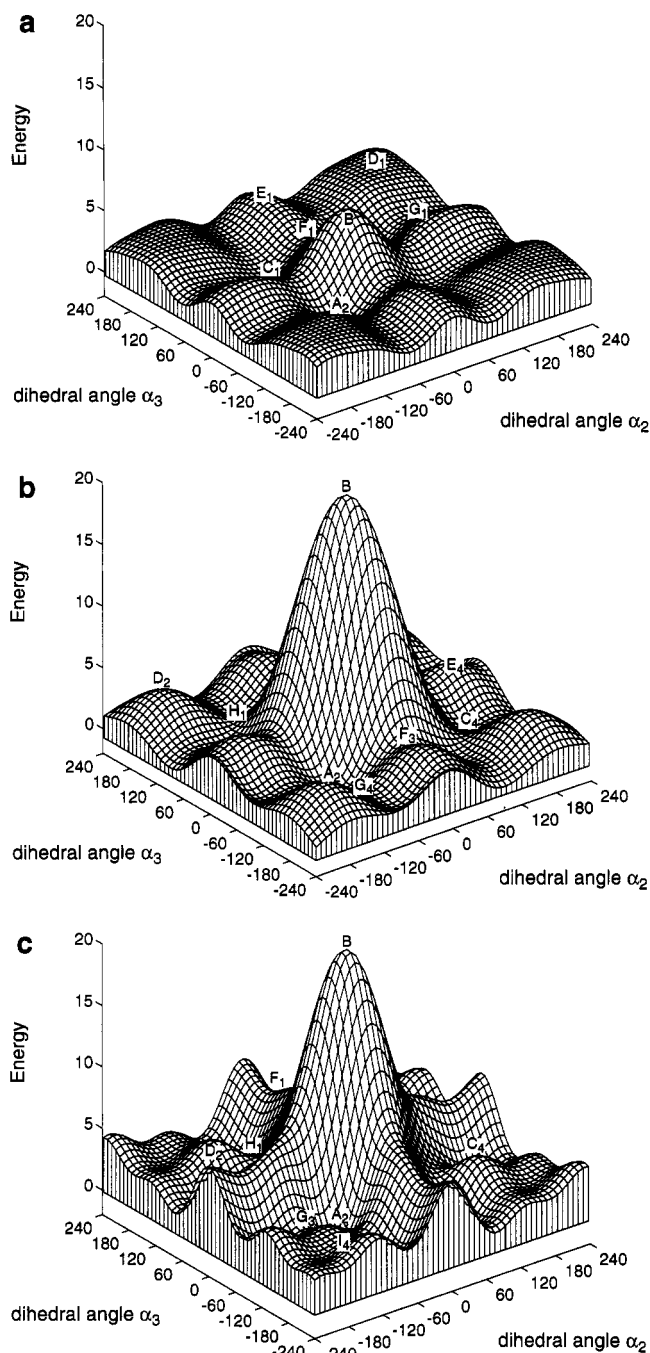


**Figure 5.** Perspective three-dimensional drawings of the  $\alpha_2, \alpha_3$ -conformational energy surface of the dimethyl phosphate (DMP) anion: (a) PM3 surface, (b) HF/3-21G(\*) surface, and (c) HF/6-31+G\*/HF/3-21G(\*) surface. Angles are in degrees and energies in kcal/mol. Stationary points are indicated by capital letters in bold print according to the notation given in Figure 2. Equivalent stationary points are numbered according to their appearance in the first, second, etc.,  $\alpha_2, \alpha_3$  quadrant of the conformational space. The range of  $\alpha$  values has been chosen to be  $\pm 240^\circ$  rather than  $\pm 180^\circ$  to facilitate comparison with the contour plots in Figure 4.

(transition state F) or to avoid steric repulsion (minimum C). When the second OCH<sub>3</sub> group rotates, it has to pass the +sc, -sc (-sc, +sc) form H, which represents a small rotational barrier in a shallow surface region (vide infra). As soon as H is passed, the first OCH<sub>3</sub> group swings into an ac position and the second C minimum is reached. Then, the actual rotation of the second OCH<sub>3</sub> group through the plane P-O1-O2 can begin. Since dihedral angles of 140–150° are not possible in a five-membered ring, the flip-flop rotation predicted by HF/3-21G(\*) is not parallel to pseudorotation of a ring. The barrier of

flip-flop rotation is determined by the energy of F, which increases from 1.4 (PM3) to 3.0 (HF/3-21G\*), Table 1) and 5.6 kcal/mol (HF/6-31+G\*, Figure 4c).

DMP can carry out another flip-flop rotation of lower energy when following the path A<sub>1</sub>-G<sub>1</sub>-C<sub>2</sub>-H<sub>1</sub>-C<sub>1</sub>-G<sub>4</sub>-A<sub>2</sub>-G<sub>3</sub>-C<sub>4</sub>-H<sub>2</sub>-C<sub>3</sub>-G<sub>2</sub>-A<sub>1</sub> (path 2) that surrounds the local maximum D<sub>1</sub> (compare with Figure 4 and Scheme 1). This path involves outwardly directed flip-flop rotations of the OCH<sub>3</sub> groups leading to ap forms and, therefore, has no relationship to conformational processes observed for five-membered rings. The barrier of the outwardly directed flip-flop rotations is just 1 kcal/mol (energy of transition states G, Table 1) at all levels of theory used. Therefore, this rotational process should be clearly the preferred rotational mode of DMP. Inspection of Figure 4b reveals that path 2 is actually located in an energy basin that in its middle has a small energy hill of 3 kcal/mol (local maximum D) and that is densely populated by DMP anion forms of low energy (Figures 4b and 5b). At the PM3 level, this energy basin is only weakly pronounced since the conformational energy surface is rather flat (Figure 5a), while at the HF/6-31+G\* level, the basin is more extended with a small plateau of 3–4 kcal/mol in its center.

Hence, the flip-flop rotation circumventing the local maximum D is predicted to be the preferred conformational process of the DMP anion. Any other rotational process following one of the minimum energy paths indicated in Figure 4 leads to transition state F and, therefore, has to surmount an energy barrier of 3–6 kcal/mol. Furthermore, we can predict that DMP or any molecule containing the DMP unit will preferentially populate the region A<sub>1</sub>-G<sub>1</sub>-C<sub>2</sub>-H<sub>1</sub>-C<sub>1</sub>-G<sub>4</sub>-A<sub>2</sub>-G<sub>3</sub>-C<sub>4</sub>-H<sub>2</sub>-C<sub>3</sub>-G<sub>2</sub>-A<sub>1</sub> clustering close to the global minima A<sub>1</sub> and A<sub>2</sub> (Figures 4 and 5).

*Fourier Analysis of the Conformational Potential.* The conformational potential of a single rotor can be approximated with a truncated Fourier expansion containing the three Fourier terms  $V_1$ ,  $V_2$ , and  $V_3$ :

$$V(\alpha) = V_0 + V_1(1 - \cos \alpha) + V_2(1 - \cos 2\alpha) + V_3(1 - \cos 3\alpha) \quad (1)$$

where  $V_0$  adjusts the zero level and  $V_1$ ,  $V_2$ , and  $V_3$  describe  $\alpha$ -dependent electronic effects that result from interactions between bond dipoles ( $V_1$ ), hyperconjugative or anomeric effects ( $V_2$ ), and bond staggering (second-order hyperconjugation effects,  $V_3$ ). For a more accurate description of the rotational potential of a single rotor molecule, eq 1 has to be extended to where  $m$  may take a finite or in the limit an infinite value. The

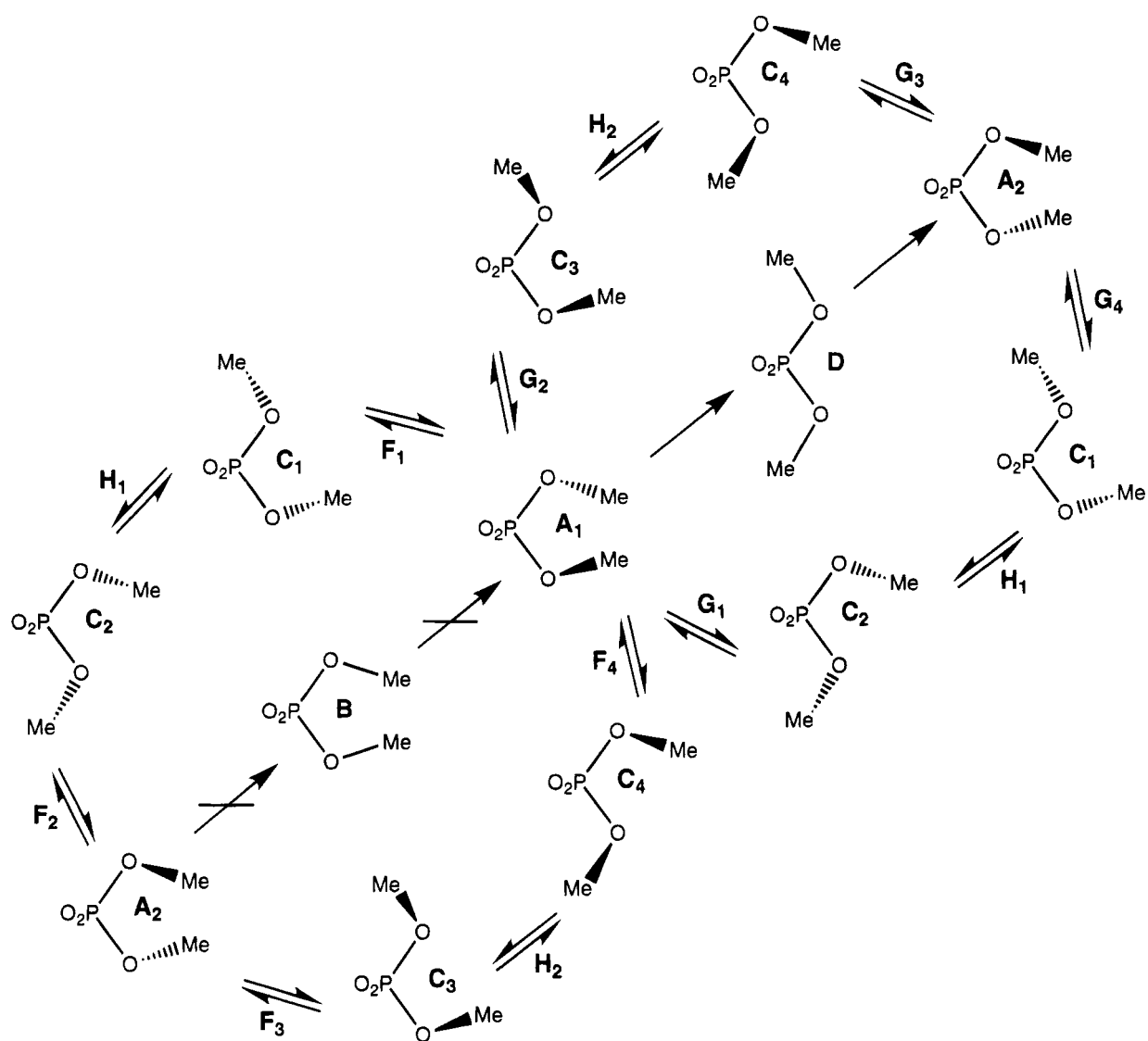
$$V(\alpha) = \sum_{k=0}^m (V_k^c \cos k\alpha + V_k^s \sin k\alpha) \quad (2)$$

Fourier description of a single rotor molecule can readily be expanded to a double rotor molecule using eq 3:

$$V(\alpha_1, \alpha_2) = \sum_{k=0}^m \sum_{l=0}^n (V_{kl}^{cc} \cos k\alpha_1 \cos l\alpha_2 + V_{kl}^{cs} \cos k\alpha_1 \sin l\alpha_2 + V_{kl}^{sc} \sin k\alpha_1 \cos l\alpha_2 + V_{kl}^{ss} \sin k\alpha_1 \sin l\alpha_2) \quad (3)$$

Previous investigations by Cremer<sup>25</sup> have shown that a satisfactory Fourier expansion for a geminal double rotor such as DMP

SCHEME 1



is of the form

$$\begin{aligned}
 V(\alpha_2, \alpha_3) = & V_{00} + V_{10}(2 - \cos \alpha_2 - \cos \alpha_3) + V_{20}(2 - \\
 & \cos 2\alpha_2 - \cos 2\alpha_3) + V_{30}(2 - \cos 3\alpha_2 - \cos 3\alpha_3) + \\
 & V_{11}^{cc} \cos \alpha_2 \cos \alpha_3 + V_{22}^{cc} \cos 2\alpha_2 \cos 2\alpha_3 + \\
 & V_{11}^{ss} \sin \alpha_2 \sin \alpha_3 + V_{22}^{ss} \sin 2\alpha_2 \sin 2\alpha_3 + \\
 & V_{12}(\cos \alpha_2 \cos 2\alpha_3 + \cos 2\alpha_2 \cos \alpha_3 - \sin \alpha_2 \sin 2\alpha_3 - \\
 & \sin 2\alpha_2 \sin \alpha_3) \quad (4)
 \end{aligned}$$

where the terms  $V_{10}$ ,  $V_{20}$ , and  $V_{30}$  cover the basic electronic effects influencing rotation<sup>33</sup> and the  $V_{kl}$  terms describe couplings between the two rotors and their electronic effects.

The conformational energy surface of the DMP anion shown in Figures 4 and 5 were obtained by fitting 17 calculated energy points corresponding to 17 unique conformers to eq 4 with a least-squares minimization approach. This procedure led to a correlation coefficient  $r^2 = 0.999$  for all three ab initio surfaces and a standard deviation  $\sigma$  of 0.16–0.24 kcal/mol (Table 3). For PM3, the result of the Fourier analysis was less satisfactory yielding  $r^2 = 0.949$  and  $\sigma = 0.51$  kcal/mol (Table 3). As indicated in Table 3, each Fourier term in eq 4 adds to the conformational energy surface of DMP a special feature. For example,  $V_{00}$  reflects the flatness (PM3) or steepness (ab initio)

of the surface, the Fourier terms  $V_{10}$ ,  $V_{11}^{cc}$ , and  $V_{12}$  shape the maxima, terms  $V_{20}$ ,  $V_{11}^{ss}$ ,  $V_{22}^{ss}$ , and  $V_{12}$  describe global and local minima, while  $V_{22}^{cc}$  is responsible for the occurrence of saddle points F and G. Since each Fourier term represents an electronic effect, the magnitude of coefficients  $V_{kl}$  indicates the importance of a particular electronic effect and its contribution to specific features of the conformational energy surface.

The Fourier coefficients listed in Table 3 reveal that at the ab initio level dipole–dipole interactions between OCH<sub>3</sub> and PO bond dipoles ( $V_{10}$ ) and between the two CO bond dipoles ( $V_{11}^{cc}$ , and  $V_{11}^{ss}$ ) dominate the rotational potential of DMP. Actually, the interaction energy between two bond dipoles  $\mu_a$  and  $\mu_b$  can be approximated by

$$\begin{aligned}
 E(DD)_{ab} &= \frac{-\mu_a \mu_b}{r_{ab}^3} (2 \cos \omega_a \cos \omega_b - \sin \omega_a \sin \omega_b \cos(\alpha_a - \alpha_b)) \quad (5)
 \end{aligned}$$

where  $r$  is the distance between the dipoles,  $\omega$  gives the deviation from a parallel alignment of the dipoles, and  $\alpha_a - \alpha_b$  is the rotational angle difference between the bond dipoles. Hence, the interaction energy is proportional to the term  $\cos(\alpha_a - \alpha_b) = \cos \alpha_a \cos \alpha_b - \sin \alpha_a \sin \alpha_b$ , which is split in eq 4 into a  $\cos(V_{11}^{cc})$  and  $\sin$  part ( $V_{11}^{ss}$ ) to account for the more compli-



**TABLE 3: Fourier Analysis of the  $V(\alpha_2, \alpha_3)$  Conformational Surface of the Dimethyl Phosphate (DMP) Anion Calculated at Various Levels of Theory (Compare with Eq 4)<sup>a</sup>**

	PM3	3-21G(*)	6-31G**/3-21G(*)	6-31+G**/3-21G(*)	comments
$V_{00}$	4.75	13.30	15.66	16.04	determines flatness (steepness) of surface
$V_{10}$	-0.16	-3.09	-2.88	-2.88	establishes maximum B and differentiates between B and D
$V_{20}$	-0.89	-1.66	-1.67	-1.68	establishes minima A and C; adds to the maxima B, D, and E
$V_{30}$	-0.32	-0.09	-0.90	-1.01	differentiates between B and D; shifts positions of A and D to smaller $\alpha$ values
$V_{11}^{cc}$	0.67	4.15	3.29	3.08	adds to the maxima at B and D
$V_{22}^{cc}$	0.17	0.64	0.43	0.27	establishes saddle points F and G
$V_{11}^{ss}$	-0.09	-1.61	-1.46	-1.44	differentiates between global (A) and local minima (C)
$V_{22}^{ss}$	-0.14	-0.86	-0.90	-0.86	shifts A closer to B; splits C in two parts and establishes saddle point H
$V_{12}$	0.30	1.01	0.83	0.64	differentiates between B and D; establishes minimum A; gives B elliptic form
$\sigma$	0.51	0.24	0.17	0.16	
$r^2$	0.949	0.999	0.999	0.999	

<sup>a</sup> Fourier coefficients  $V_{kl}$  and standard deviations  $\sigma$  in kcal/mol,  $r^2$  is the correlation coefficient.

**TABLE 4: Total Atomic Charges of the Global Minimum of the Dimethyl Phosphate (DMP) Anion (A) Calculated with Different Methods**

atom/group <sup>a</sup>	PM3	3-21G(*)	6-31G**/3-21G(*)	6-31+G**/3-21G(*)
P	2.04	1.51	1.56	2.58
O3	-0.94	-0.77	-0.82	-1.10
O1	-0.66	-0.75	-0.74	-0.87
C	0.16	-0.26	-0.15	-0.36
H1	-0.04	0.15	0.12	0.15
H2	-0.01	0.21	0.18	0.22
H3	-0.04	0.16	0.13	0.16
CH <sub>3</sub>	0.08	0.26	0.28	0.17

<sup>a</sup> For atom labels, see Figure 1a.

cated  $\alpha_2, \alpha_3$  dependence of the dipole-dipole interaction energy due to changes in the dipole moment values and the alignment of the bond dipoles during rotation of the OCH<sub>3</sub> groups.<sup>25</sup> Both  $V_{10}$ ,  $V_{11}^{cc}$ , and  $V_{11}^{ss}$  are rather large (-3.1, 4.1, -1.6, HF/3-21G(\*), Table 3), indicating that PO and OCH<sub>3</sub> bond dipole moments are also large and lead to considerable interactions. This is confirmed by the calculated atomic (group) charges listed in Table 4, which suggest large PO and OMe dipole moments. However, at the PM3 level, the charge of a CH<sub>3</sub> group (0.08 electron) is just one-third of that calculated at the HF/3-21G(\*) level (0.26, Table 4), thus leading to a much lower bond dipole moment. This effect is even increased by a shortening of the CO distance at the PM3 level (1.37 versus 1.44 Å, Table 2), which is parallel to or a consequence of an unreasonably long PO bond length (1.77 vs 1.63 Å, Table 2).

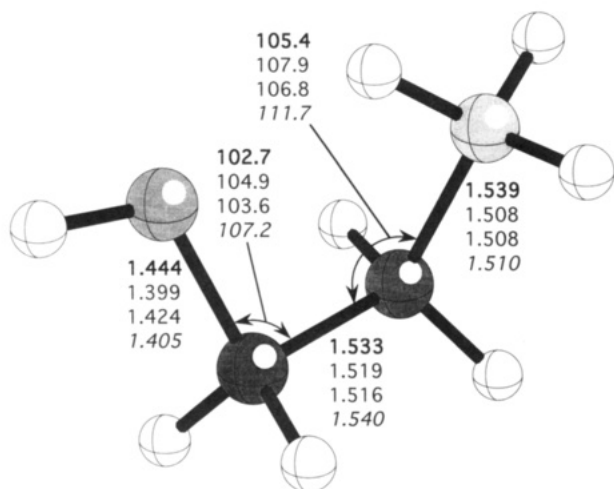
We conclude that the basic appearance of the PM3 conformational surface is a result of underestimating dipole-dipole interactions. This, in turn, can be directly traced to an underestimation of charge separation in the CO bonds, probably coupled to an exaggeration of the PO bond lengths. From experimental investigations it is known that the PO(C) bond lengths of a phosphate group are about 1.60 Å (standard deviation of 0.03).<sup>34</sup> HF/3-21G(\*) comes close to this value (1.63 Å). The inclusion of polarization functions at all heavy atoms rather than just the P atom leads to a slight increase rather than a decrease of the PO(C) bond lengths (1.64 Å, HF/6-31G\*, Figure 3), thus indicating that the basis set is actually not s,p-saturated and, in addition, lacks diffuse functions for the correct description of the anionic charge distribution. As a consequence, MP2/6-31G\* leads to additional lengthening of the PO(C) bond (1.68 Å, Figure 3), which results from the known tendency of MP2 to increase bond lengths artificially if the basis set used is too small for the problem to be investigated. In the present case, use of MP2/6-311G(pd + diffuse sp) would be more appropriate to get reliable PO(C) bond lengths. We conclude that, because of a fortuitous cancellation of basis set and correlation errors, HF/3-21G(\*) geometries are the most reliable ab initio geometries, which presently can be obtained at relatively low cost.

In view of a discrepancy of 0.17 Å between experimental and PM3 values (1.77 Å, Table 2), the geometry description of the DMP anion at the ab initio level is much better than that at the semiempirical level. Therefore, the peculiar appearance of the PM3 conformational surface can be traced down to the wrong description of the PO bonds probably because of insufficient parametrization of the P atom.

Another feature of the PM3 surface, namely the somewhat larger stability of minima C as compared to minima A (0.4 kcal/mol, Table 1), is a direct result of the underestimation of dipole-dipole effects at the PM3 level of theory. The term  $V_{11}^{ss}$  describes dipole-dipole interactions in the four possible DMP anion forms with  $\alpha_2, \alpha_3 = \pm 90^\circ$  that influence the energy difference between forms A and C. Since the coefficient  $V_{11}^{ss}$  is calculated to be -1.4 to -1.6 at the ab initio level, there is an energy difference of 0.7-1.6 kcal/mol in favor of A. At the PM3 level,  $V_{11}^{ss}$  is negligibly small and, therefore, the two minima A and C have comparable energies. The exact location of C (Table 1) leads to a slight preference of this DMP anion form at the PM3 level, which must be considered as an artifact of the method used as described above. The -sc,+sc (+sc,-sc) conformer C has not been observed experimentally.

Contrary to other geminal double rotors that possess heteroatoms, the anomeric effect ( $V_{20}$ ) is less important for the rotational potential of DMP than dipole-dipole interactions as is revealed by the magnitude of the Fourier coefficients ( $V_{20} = -1.7$ ,  $V_{22}^{cc} = 0.6$ ,  $V_{22}^{ss} = -0.9$ ; HF/3-21G(\*)) listed in Table 3. The stability of the minimum forms A and C results from anomeric delocalization<sup>35-37</sup> of oxygen lone pair electrons into the  $\sigma^*$  orbital of the adjacent PO(CH<sub>3</sub>) bond. This delocalization is effective if the energy difference between the lone pair and the  $\sigma^*$  orbital is relatively small and the two orbitals overlap strongly. The latter requirement is fulfilled if the adjacent PO bond is colinear with the electron lone pair, which is best accomplished in the sc conformations A and C (see Figure 2).

Equation 4 includes the terms  $V_{22}^{cc}$  and  $V_{22}^{ss}$  to describe the coupling between the two anomeric effects possible for the DMP anion. Although the importance of these terms is smaller than those of the dipole-dipole interaction terms, they cannot be neglected in the discussion since they account for the exact location of minimum A ( $V_{22}^{ss}$ ), determine the structure of the surface at C (splitting into two equivalent local minima C with an intermediate saddlepoint H,  $V_{22}^{ss}$ ), and are responsible for the location of saddle points F and G ( $V_{22}^{cc}$ ). The coupling between the anomeric effect and dipole interactions is covered by the term  $V_{12}$  (1.0 at HF/3-21G(\*), Table 3), which, although not very large, is important for the fine structure of the conformational energy surface as becomes obvious by drawing this term and comparing it with that in Figure 4. There is a small contribution resulting from bond staggering ( $V_{30}$ , Table 1), but all coupling terms of the type  $V_{3l}$  can be neglected.



$\alpha_4 = 170.0$	$\alpha_5 = 41.7$	HF/3-21G(*)
$\alpha_4 = 173.3$	$\alpha_5 = 48.5$	HF/6-31G*
$\alpha_4 = 176.3$	$\alpha_5 = 48.2$	MP2/6-31G*
$\alpha_4 = 146.4$	$\alpha_5 = 50.9$	PM3

**Figure 6.** Minimum energy conformation of the 2-ammonioethanol (AME) cation. HF/3-21G(\*) values for heavy-atom bond lengths and angles are given in bold print (HF/6-31G\*, normal, MP2/6-31G\*, normal, PM3, italics).

The Fourier analysis shows that a reliable description of the conformational energy surface of the DMP anion critically depends on a reliable calculation of the charge distribution in the anion. This, of course, is best done with the 6-31+G\* basis set, which contains both diffuse functions to describe diffuse charge distributions of an anion and polarization functions to describe charge separation in polar heavy atom bonds. It has been established by investigations on hypervalent molecules that changes in geometry parameters are minimal when going from the HF/3-21G(\*) to the HF/6-31+G\* level of theory.<sup>22</sup> Inconsistencies resulting from using HF/3-21G(\*) geometries for HF/6-31+G\* single point calculations will be small, and therefore, the best account of the rotational surface of DMP should be provided at the HF/6-31+G\*/HF/3-21G(\*) level (Figures 4c and 5c).

**3.2. Conformational Energy Surface of AME.** The conformational energy surface of the AME cation possesses  $C_2$  symmetry, which is confirmed at the PM3 (Figure 7a) and HF/3-21G levels of theory (Figure 7b,c). Again, the PM3 surface is much flatter than the ab initio surface (compare Figure 8a with Figure 8b,c). As in the case of DMP, this results from an underestimation of dipole-dipole interactions within the molecule at the PM3 level and is the reason why we will discuss in the following just the HF/3-21G conformational energy surface of the AME cation.

The overall features of the conformational energy surface of the AME cation are much more complex than those of the DMP surface (which of course has to do with the lowering of symmetry from  $C_{2v}$  to  $C_2$ ), but with regard to the central global maximum B occupied by the sp,sp form, both surfaces are similar. The perspective three-dimensional drawing of the surface given in Figure 8b reveals that B actually corresponds to a broad peak or a double peak connected by an energy ridge; however, these are details of little relevance since B lies 30.6 kcal/mol (PM3, 15.9 kcal/mol; Table 5) above two symmetry-equivalent global minima A in the ap,sc region (MP2/6-31G\*,  $\alpha_4 = 176.3$ ,  $\alpha_5 = 48.2$ ; HF/6-31G\*,  $\alpha_4 = 173.3$ ,  $\alpha_5 = 48.5$ ; HF/3-21G,  $\alpha_4 = 170.0$ ,  $\alpha_5 = 41.7$ ; PM3,  $\alpha_4 = 146.4$  and  $\alpha_5 = 50.9$ ; Figure 6; compare with Figures 7 and 8). The two

minima are separated by high-energy mountains such as B,  $K_1$ , and  $K_2$  ( $\Delta E = 24$ -30 kcal/mol) that stretch out along the line  $\alpha_4 = 0^\circ$ .

A comparison of the geometry of the minimum energy conformation A of AME obtained by ab initio and PM3 calculations (Figure 6 and Table 6) shows some remarkable differences. The bond angles O2C2C3 (102.7°) and C2C3N (105.4°) of the ab initio structure are significantly smaller than those obtained by PM3, while the bond lengths of the O2C2 bond (1.44 Å) and particularly the C3N<sup>+</sup> bond (1.54 Å) are longer, indicating that PM3 does not correctly account for the bond polarization and charge distribution (compare Table 8) and thus underestimates dipole-dipole interactions in the AME cation. In crystal structures of phosphoethanolamines,  $\alpha_4$  ranges from 106° to 256° (average 173°) and  $\alpha_5$  from 54° to 96° (average 69.5°). The larger value of  $\alpha_5$  probably has to be attributed to intermolecular electrostatic forces in the crystal lattice which to some extent counterbalance the strong intramolecular electrostatic interactions in AME.

In the  $\alpha_4, \alpha_5$  energy surface, there are also some local minima, namely C (12.7 kcal/mol) and D (14.9 kcal/mol, 3-21G), which are occupied by ap,ap (C) and -sc,ap (D) forms. The local minima can be reached by following the minimum energy paths shown in Figure 7 in the form of dashed lines.

At the 6-31G\* level, the relative energy of C decreases to 7.3 kcal/mol, but this is still too large to lead to a significant population of C in an equilibrium situation.

**Preferred Conformational Processes of the AME Cation.** There is a flip-flop rotation path (path 1 in the case of the DMP anion) surrounding B (see Figure 7b), but transition states F are much too high in energy (HF/3-21G, 21.8; HF/6-31G\*, 14.7 kcal/mol; Table 5) to make this rotational mode likely. Several minimum energy paths lead from the global minima A to local minima C and D located between the maxima K and L (Figure 8b). The path to D leads through a transition state in the vicinity of maximum L, with an energy higher than 18 kcal/mol, and is therefore energetically unfavorable (see Figure 7b). In the case of C, transition state I ( $\alpha_4 = 166.3^\circ$ ,  $\alpha_5 = 127.0^\circ$ ; Table 5) has to be crossed, which has relative energies of 15.2 (HF/3-21G) and 9.3 kcal/mol (HF/6-31G\*, Table 5), respectively. Stationary points C and I lie on path  $A_1-I_1-C_1-C_2-I_2-A_2$  (path 2). Path 2 corresponds to a rotation at the CC bond from  $\alpha_5 = 42^\circ$ -180° and 318° (= -42°) with the OH group just swinging from  $\alpha_4 = 170^\circ$ -190°. One can consider the region between  $C_1$  and  $C_2$  as just one energy valley stretching out at the position of the ap,ap form, and the splitting up in two minima  $C_1$  and  $C_2$  is actually a numerical error which originates from the Fourier fit (compare Table 5 and Figure 7b). Hence, the rotational barrier of path 2 is given by the energy of I, which in view of a HF/6-31G\* value of 9.3 kcal/mol can be surmounted by the molecule at room temperature.

Although some AME cations may populate the local minima C, the majority of AME molecules will populate a relative narrow region defined by  $120^\circ \leq \alpha_4 \leq 240^\circ$  and  $-60^\circ \leq \alpha_5 \leq 60^\circ$ , which is the location of the two global minima  $A_1$  and  $A_2$ . In Figures 7c and 8c, this region is shown in both the form of a contour line diagram and a perspective three-dimensional drawing so that it is possible to visualize the most important conformational processes of the AME cation. AME can easily rotate from the minimum conformation  $A_1$  to the conformation  $A_2$  by passing transition state G (HF/3-21G, 2.5 kcal/mol; HF/6-31G\*, 5.1 kcal/mol; Table 5), which corresponds to a ap,sp conformer of the AME cation (Figure 7c). In summary, the conformational flexibility of the AME cation is much lower than that of the DMP anion. A 360° rotation at the CO bond

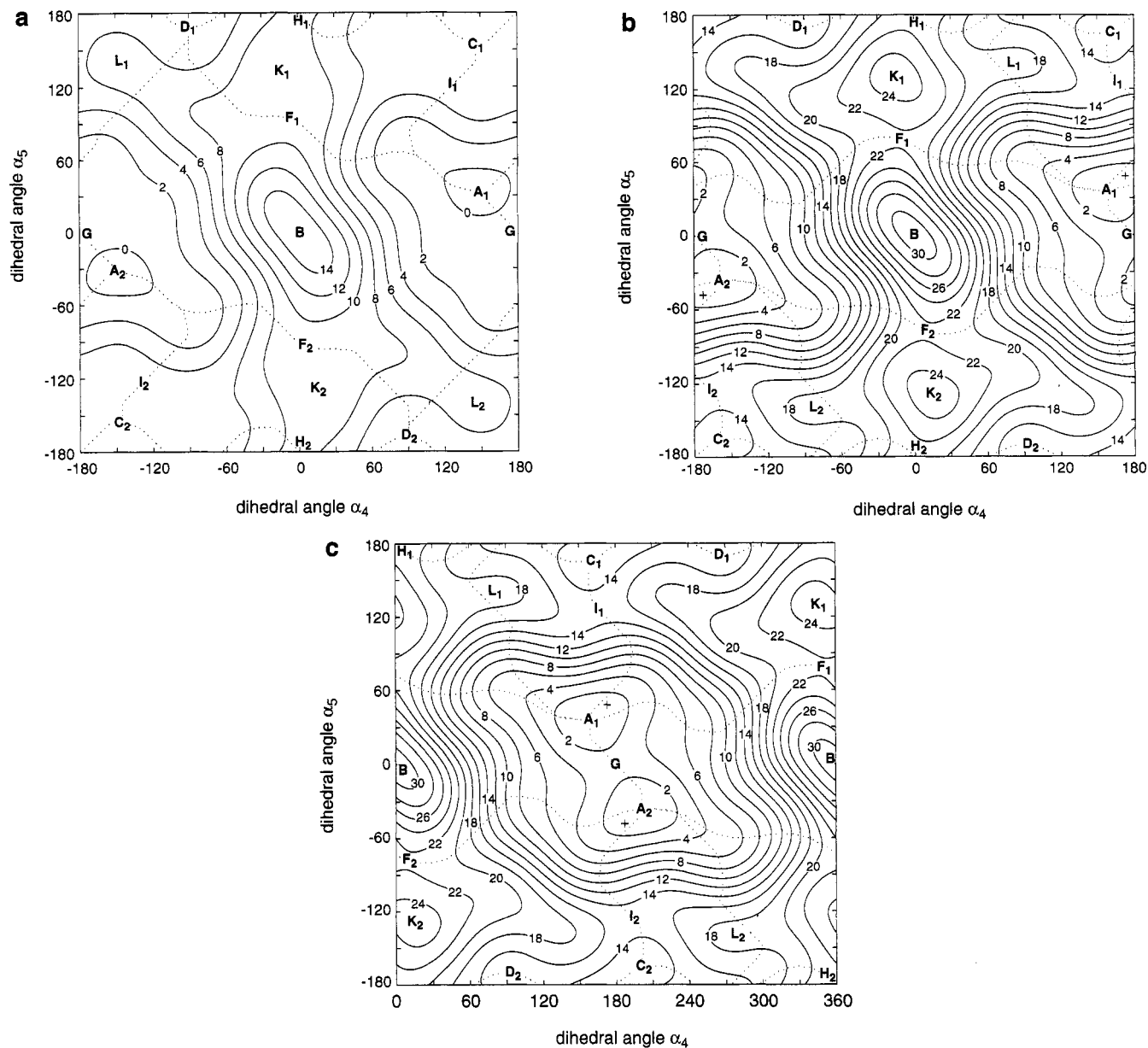


**Figure 7.** Contour line diagram of the  $\alpha_4, \alpha_5$ -conformational energy surface of the 2-ammonioethanol (AME) cation: (a) PM3 surface, (b) HF/3-21G surface in the region  $-180^\circ \leq \alpha_4, \alpha_5 \leq 180^\circ$ , and (c) HF/3-21G surface in the regions  $0^\circ \leq \alpha_4 \leq 360^\circ$  and  $-180^\circ \leq \alpha_5 \leq 180^\circ$ . Contour levels in kcal/mol are given in small print. Stationary points are indicated by capital letters in bold print, following as far as possible the labeling of stationary points in Figure 4. Minimum energy paths connecting global and local energy minima as well as intermediate saddle points are given by dashed lines. In the case of the HF/3-21G surface, two different ranges of  $\alpha$ -values have been chosen to make a direct comparison with the DMP anion surface possible (b) and to show the region with the two global minima (c).

is excluded at room temperature because of barriers as high as 21.7 kcal/mol (HF/3-21G) or 14.7 kcal/mol (HF/6-31\*, saddle point F). Just a large-amplitude vibration of the OH group between  $\alpha_4 = 120^\circ$  and  $240^\circ$  is possible where the molecule stays essentially in the ap form. The preferred rotational mode at the CC bond is a back-and-forth swinging between two gauche conformations with  $\alpha_5 = \pm 48^\circ$  (HF/6-31G\*,  $\Delta E = 5.1$  kcal/mol). However, a complete rotation at the CC bond is also possible since the energy barrier is just 9.3 kcal/mol at HF/6-31G\*. While the conformational flexibility of the DMP anion is characterized by a strong coupling between the two rotor groups, rotor coupling is largely excluded in the case of the AME cation.

**Fourier Analysis of the Conformational Potential.** The conformational energy surfaces of the AME cation were fitted to the Fourier series expansion given in eq 3 with  $k, l \leq 3$ . After eliminating those Fourier terms with small Fourier

coefficients, expansion 6 was obtained. Expansion 6 differs

$$\begin{aligned}
 V(\alpha_4, \alpha_5) = & V_{00} + V_{10}(1 - \cos \alpha_4) + V_{20}(1 - \cos 2\alpha_4) + \\
 & V_{30}(1 - \cos 3\alpha_4) + V_{01}(1 - \cos \alpha_5) + V_{03}(1 - \cos 3\alpha_5) + \\
 & V_{11}^{ss} \sin \alpha_4 \sin \alpha_5 + V_{33}^{ss} \sin 3\alpha_4 \sin 3\alpha_5 + \\
 & V_{11}^{css} (\cos \alpha_4 \cos \alpha_5 - \sin \alpha_4 \sin \alpha_5) + \\
 & V_{22}^{css} (\cos 2\alpha_4 \cos 2\alpha_5 - \sin 2\alpha_4 \sin 2\alpha_5) + \\
 & V_{12} (\cos \alpha_4 \cos 2\alpha_5 + \cos 2\alpha_4 \cos \alpha_5 - \sin \alpha_4 \sin 2\alpha_5 - \\
 & \sin 2\alpha_4 \sin \alpha_5) \quad (6)
 \end{aligned}$$

from expansion 4 because the AME cation can adopt either  $C_1$  or  $C_s$  symmetry while the highest symmetry of the DMP anion is  $C_{2v}$ . Fitting the HF/3-21G points to eq 6 leads to a correlation coefficient  $r^2 = 0.997$  and a standard deviation  $\sigma$  of 0.55 kcal/

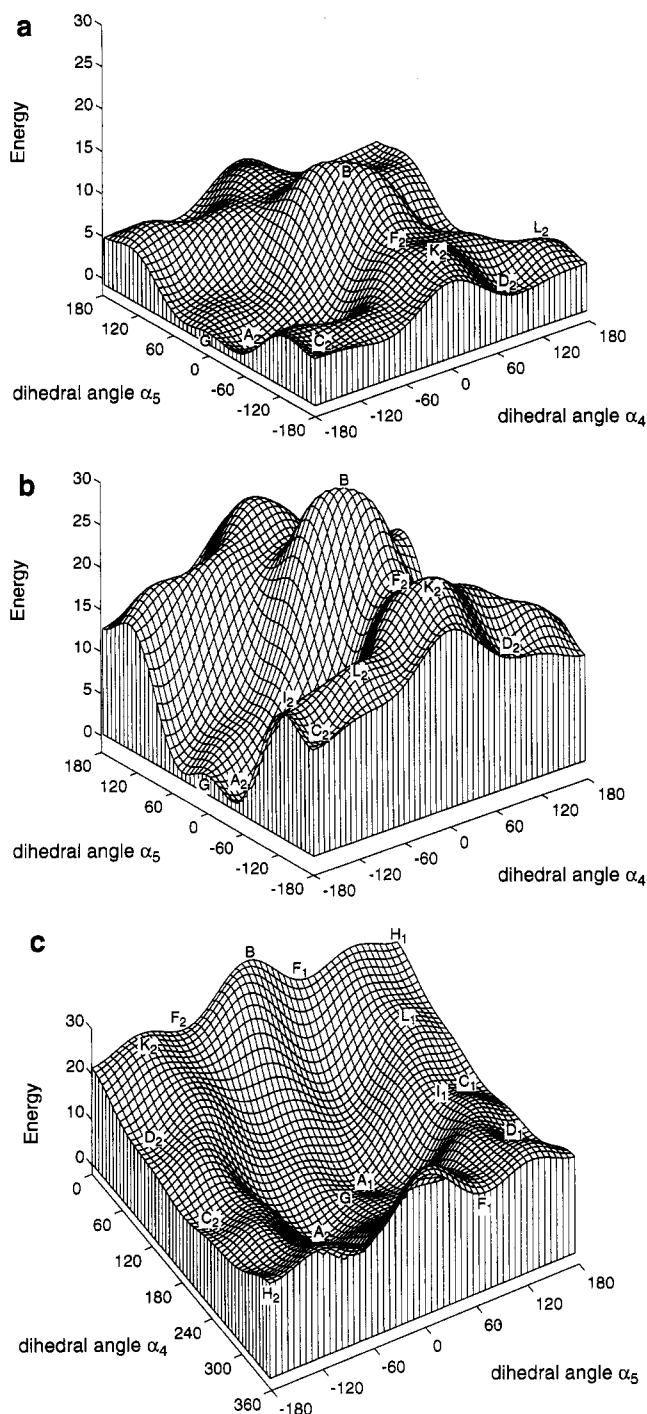
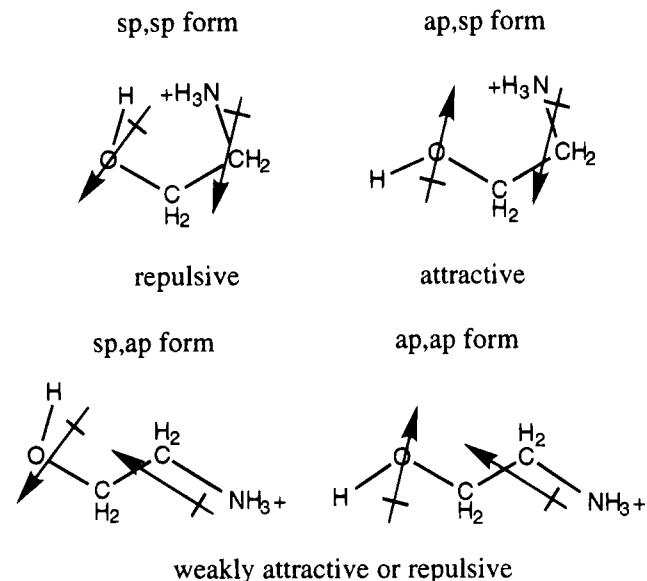


**Figure 8.** Perspective three-dimensional drawings of the  $\alpha_4, \alpha_5$ -conformational energy surface of the 2-aminoethanol (AME) cation: (a) PM3 surface, (b) HF/3-21G surface in the region  $-180^\circ \leq \alpha_4, \alpha_5 \leq 180^\circ$ , and (c) HF/3-21G surface in the region  $0^\circ \leq \alpha_4 \leq 360^\circ$  and  $-180^\circ \leq \alpha_5 \leq 180^\circ$ . Angles are in degrees and energies in kcal/mol. Stationary points are indicated by capital letters in bold print. In the case of the HF/3-21G surface, two different ranges of  $\alpha$  values have been chosen to make a direct comparison with the DMP anion surface possible (b) and to show the region with the two global minima (c).

mol. For the PM3 surface,  $r^2 = 0.983$  and  $\sigma = 0.78$  kcal/mol were obtained.

The Fourier coefficients listed in Table 7 indicate that dipole-dipole interactions dominate the rotational behavior of the AME cation. For the OH group, the local dipole moment is largely parallel to that of the  $\text{CH}_2\text{NH}_3^+$  group if  $\alpha_4 = \alpha_5 = 0^\circ$ . However, if the OH group rotates into the ap position, the two dipole moments will be antiparallel and, accordingly, attract each

other. Dipole-dipole repulsion in the sp,sp form is rather strong as is reflected by  $V_{10} = -7.2$  (Table 7). Rotation of the  $\text{CH}_2\text{-NH}_3^+$  group from the sp to the ap position decreases dipole-dipole attraction in the sp,ap form. As a consequence, the



corresponding dipole term in expansion 6,  $V_{01}$ , is positive (3.8, Table 7). While  $V_{10}$  builds up the central maximum B,  $V_{01}$  reduces the height of B to some extent. Coupling between the dipole terms ( $V_{11}^{ss} = 1.6$  and  $V_{11}^{ccss} = 5.0$ , Table 7) again adds to the height of maximum B and, in addition, creates a region of relative high energy along the direction  $\alpha_4 = -\alpha_5$ .

There is anomeric delocalization at the site of the OH group ( $V_{20} = -1.4$ ) but, of course, not for the  $\text{CH}_2\text{NH}_3^+$  rotor ( $V_{02} = 0$ ). The anomeric effect leads to the minimum at A where the exact location of A is actually determined by bond staggering terms. Bond staggering is more important for the  $\text{CH}_2\text{NH}_3^+$  rotor ( $V_{03} = -2.4$ ) than the OH rotor ( $V_{30} = -0.8$ , Table 7). Coupling of these two effects ( $V_{33}^{ss} = -1.5$ ) determines the position of the global minimum at A (HF/3-21G,  $\alpha_4 = 170^\circ$ ,  $\alpha_5 = 42^\circ$ ; HF/6-31g\*,  $\alpha_4 = 173^\circ$ ,  $\alpha_5 = 48^\circ$ ).

The Fourier coefficients listed in Table 7 reveal that the basic failure of PM3 is again an underestimation of dipole-dipole interaction terms, which can be traced back to a wrong description of the charge distribution in AME (Table 8). PM3 localizes the positive charge at the  $\text{NH}_3^+$  group, while ab initio theory indicates that some of the positive charge is delocalized by hyperconjugative interactions to the adjacent  $\text{CH}_2$  groups. Also, the OH group takes over considerably more negative charge (because of its electronegativity) than predicted by PM3. Accordingly, the CO bond polarity and the CO bond dipole moment are significantly larger than those given at the PM3 level.

#### 4. Conclusions

A number of important conclusions can be drawn from this work which are useful for the investigation of phospholipid head groups.

(1) The comparison of ab initio and semiempirical PM3 results reveals that, despite of extensive parametrization of PM3, this method does not provide a reliable description of the conformational tendencies of either the DMP anion or the AME cation, which are the basic units for phospholipid head groups. The source of this failure can be traced back to (a) an insufficient parametrization of hypervalent P in the case of the DMP anion;

TABLE 5: Calculated Energies for Selected Conformations of the 2-Ammonioethanol (AME) Cation<sup>a</sup>

conf <sup>b</sup>	sym	PM3			sym	3-21G			6-31G*/3-21G
		$\alpha_4$	$\alpha_5$	$\Delta E$		$\alpha_4$	$\alpha_5$	$\Delta E$	
A <sub>1</sub> <sup>c</sup>	C <sub>1</sub>	146.4	50.9	0.0	C <sub>1</sub>	170.0	41.7	0.0	0.0
B	C <sub>s</sub>	0.0	0.0	15.9	C <sub>s</sub>	0.0	0.0	30.6	23.7
C <sub>1</sub>	C <sub>1</sub>	179.6	179.7	5.5	C <sub>1</sub>	180.0	180.0	12.7	7.3
D <sub>1</sub>	C <sub>1</sub>	-90.0	169.0	4.2 <sup>c</sup>	C <sub>1</sub>	-96.9	171.3	14.9 <sup>c</sup>	
F <sub>1</sub>	C <sub>1</sub>	-3.2	93.3	9.7 <sup>c</sup>	C <sub>1</sub>	-19.5	75.7	21.8	14.7
G <sub>1</sub>	C <sub>1</sub>	180.0	0.0	1.4	C <sub>1</sub>	180.0	0.0	2.5	5.1
H <sub>1</sub>	C <sub>1</sub>	0.0	180.0	8.9	C <sub>1</sub>	0.0	180.0	21.5	14.3
I <sub>1</sub>	C <sub>1</sub>	130.0	123.8	5.1 <sup>c</sup>	C <sub>1</sub>	166.3	127.0	15.2	9.3
K <sub>1</sub>	C <sub>1</sub>	-14.3	130.6	10.0 <sup>c</sup>	C <sub>1</sub>	-15.6	130.2	25.0 <sup>c</sup>	
L <sub>1</sub>	C <sub>1</sub>	-142.9	138.8	7.2 <sup>c</sup>	C <sub>1</sub>	80.9	139.8	18.7 <sup>c</sup>	

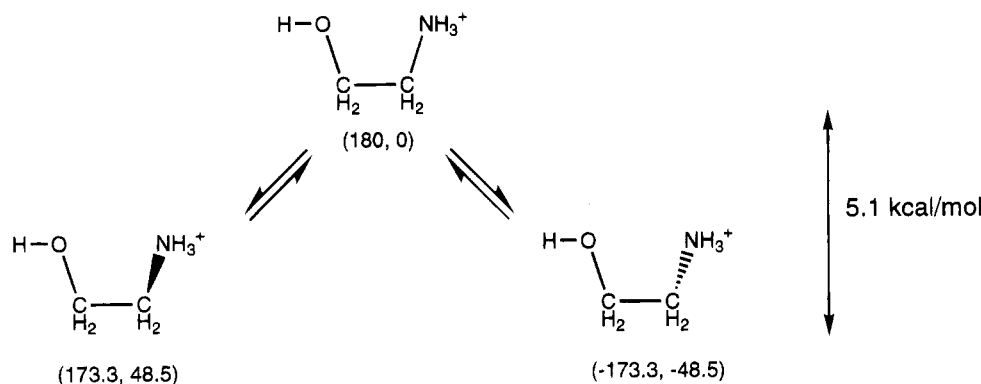
<sup>a</sup> Dihedral angles  $\alpha_i$  in degrees, relative energies in kcal/mol. All energy data relative to the energy of conformer A. Heat of formation of A: 102.5 kcal/mol (PM3); absolute energies of A: -208.33093 au (HF/3-21G), -209.46672 au (HF/6-31G\*/HF/3-21G). <sup>b</sup> For the notation of conformers, see Figure 7. <sup>c</sup> Dihedral angles and energy values derived from the Fourier expansion, eq 6.

TABLE 6: Calculated Geometry Parameters for Selected Conformers of the 2-Ammonioethanol (AME) Cation

conformer <sup>a</sup>	A <sub>1</sub>	B	C <sub>1</sub>	F <sub>1</sub>	G <sub>1</sub>	H <sub>1</sub>	I <sub>1</sub>
	A. PM3						
H1-O	0.948	0.945	0.948		0.948	0.948	
O-C2	1.405	1.398	1.401		1.407	1.395	
C2-C3	1.540	1.550	1.544		1.549	1.544	
C3-N	1.510	1.502	1.503		1.508	1.505	
H1-O-C2	108.1	112.9	107.6		107.6	110.6	
O-C2-C3	107.2	121.4	105.0		107.8	115.0	
C2-C3-N	111.7	117.6	111.7		113.8	111.1	
$\alpha_4$ (H1-O-C2-C3)	146.4	0.0	179.6		180.0	0.0	
$\alpha_5$ (O-C2-C3-N)	50.9	0.0	179.7		0.0	180.0	
	B. HF/3-21G						
H1-O	0.966	0.960	0.967	0.964	0.966	0.966	0.967
O-C2	1.444	1.438	1.428	1.432	1.444	1.428	1.431
C2-C3	1.533	1.571	1.529	1.530	1.567	1.538	1.543
C3-N	1.539	1.551	1.551	1.561	1.538	1.548	1.555
H1-O-C2	114.6	119.0	113.3	116.3	114.8	115.4	112.9
O-C2-C3	102.7	118.2	100.0	114.7	105.4	111.4	103.3
C2-C3-N	105.4	112.7	111.2	110.3	107.6	109.7	111.3
$\alpha_4$ (H1-O-C2-C3)	170.0	0.0	180.0	-19.5	180.0	0.0	166.3
$\alpha_5$ (O-C2-C3-N)	41.7	0.0	180.0	75.7	0.0	180.0	127.0

<sup>a</sup> For the notation of the conformers, see Figure 7.

## SCHEME 2



(b) an underestimation of bond polarities (CO and PO bonds); and (c) an underestimation of charge delocalization effects such as hyperconjugation and anomeric effect.

Consequences of these failures are an inaccurate description of the charge distribution in the molecule (positive charge localized at N in the AME cation), bond lengths (in particular the PO(Me) bond in the DMP anion), and other geometrical parameters. This leads to an underestimation of dipole-dipole interactions and a severe underestimation of rotational barriers for both molecules. According to PM3, both DMP anion and AME cation are highly flexible rotor molecules that can adopt, under the influence of environmental effects, almost any

rotational form possible. If this would be true, phospholipid head groups would be also conformationally very flexible and there would be almost no reason to expect certain preferred conformations. This is in contradiction with the conformational restrictions reflected by the experimental results.<sup>1</sup>

The failures of the PM3 method documented in this work will also show up in closely related semiempirical methods such as MNDO<sup>38</sup> or AM1.<sup>39</sup> Therefore, PM3 or related semiempirical methods are not reliable for the conformational description of phospholipid head groups.

(2) Ab initio theory provides a consistent description for both molecules already at the HF level of theory. Calculations show

**TABLE 7: Fourier Analysis of the  $V(\alpha_4, \alpha_5)$  Conformational Surface of the 2-Ammonioethanol (AME) Cation Calculated at Various Levels of Theory (Compare with Eq 6)<sup>a</sup>**

	PM3	3-21G	comments
$V_{00}$	10.60	22.78	determines flatness (steepness) of surface
$V_{10}$	-3.44	-7.20	builds up central maximum B
$V_{20}$	-1.36	-1.42	establishes minima A and adds to B
$V_{30}$	-0.40	-0.81	increases the difference between A and B
$V_{01}$	0.84	3.78	reduces central maximum B
$V_{03}$	-0.82	-2.38	adds to maxima at B and K, lowers points F and H
$V_{11}^{ss}$	0.59	1.56	adds to B and establishes minimum C
$V_{33}^{ss}$	-0.94	-1.53	determines the position of minimum A
$V_{11}^{ccss}$	2.76	4.95	establishes a ridge of maxima along the line $\alpha_4 = -\alpha_5$
$V_{22}^{ccss}$	0.53	0.72	establishes a ridge of maxima along the line $\alpha_4 = -\alpha_5$
$V_{12}$	0.65	1.22	differentiates between B and C; gives B elliptic form
$\sigma$	0.78	0.55	
$r^2$	0.983	0.997	

<sup>a</sup> Fourier coefficients  $V_{kl}$  and standard deviations  $\sigma$  in kcal/mol.  $r^2$  is the correlation coefficient.

**TABLE 8: Atomic Charges of the Global Minimum of the 2-Ammonioethanol (AME) Cation Calculated with Different Methods**

atom/group <sup>a</sup>	PM3	3-21G
O	-0.35	-0.71
C2	0.07	-0.10
C3	-0.30	-0.28
N	0.86	-0.85
H1	0.25	0.44
H2	0.08	0.28
H3	0.06	0.25
H4	0.13	0.32
H5	0.13	0.31
H6	0.03	0.48
H7	0.02	0.43
H8	0.01	0.44
OH	-0.10	-0.27
CH <sub>2</sub> (C2)	0.22	0.41
CH <sub>2</sub> (C3)	-0.04	0.36
NH <sub>3</sub> <sup>+</sup>	0.92	0.50

<sup>a</sup> For atom labels, see Figure 1b.

that some care has to be taken with regard to the level of geometry optimization and the basis set used. In view of the relatively large number of geometrical parameters, small errors in a partially optimized structure easily add up to substantial errors in calculated conformational energies, which makes complete geometry optimizations absolutely necessary if a consistent description of various conformations should be obtained. However, it is possible to obtain such a consistent description already with a DZ basis set. In the case of the DMP anion, HF/DZ energies have to be checked with a DZ+P+diff basis set, while in the case of the AME cation, a DZ+P basis is sufficient.

(3) Although dipole interactions are most important for the DMP anion, the location of the minimum energy conformations of the molecule are determined by anomeric delocalization effects. Accordingly, the global minimum is the location of a sc,sc conformation while the local minima are the positions of conformations such as -sc,+ac and -ac,+sc (HF/3-21G(\*)) or -sc,ap and ap,+sc (HF/6-31+G\*). In the case of the AME cation, the exact position of the global minima is more due to dipole-dipole interactions (which want to keep the molecule in an ap,sp form) and bond staggering effects (which rotate the CH<sub>2</sub>NH<sub>3</sub><sup>+</sup> group toward  $\alpha_5 = 60^\circ$ ).

(4) The DMP anion is a rather flexible geminal double rotor that can perform two different flip-flop rotations surrounding in this way either the local maximum D or the global maximum B. The first mode involves outwardly directed rotations of the OCH<sub>3</sub> group with rather small rotational barriers of just 1 kcal/mol. A relatively large energy basin that stretches around D,

from A<sub>1</sub> to A<sub>2</sub>, can be filled by DMP anion conformers with similar energy. Apart from this, the DMP anion can carry out inwardly directed flip-flop rotations with barriers of 3–6 kcal/mol, thus converting one minimum energy conformation into the other.

(5) The AME cation keeps during its preferred conformational mode the OH rotor group essentially in an ap form while the CH<sub>2</sub>NH<sub>3</sub><sup>+</sup> group swings between two sc conformations. The barrier for this process that directly leads from A<sub>1</sub> to A<sub>2</sub> via transition state G, is just 5.1 kcal/mol (HF/6-31G\*). A rotation at the CC bond in the opposite direction requires surmounting a barrier of 9.3 kcal/mol (transition states I, HF/6-31G\*). Hence, the rotational flexibility of the AME cation is largely limited to rotation at the CC bond. Contrary to the DMP anion, a conformational process with extensive rotor coupling is excluded in the case of the AME cation.

In this work, we have laid the basis for an analysis of the conformational tendencies of phospholipid head groups. It is known that conformational effects are largely additive in acyclic molecules apart from a coupling between effects of directly adjacent rotor groups. Hence, we can expect that the conformational behavior of phosphoethanolamine or phosphocholine can be directly derived from the conformational preferences of the DMP anion and the AME cation calculated in this work. Any deviation from these predictions will indicate new effects between the DMP and the AME unit such as H-bonding, charge attraction, etc., that are only possible for the total head group. The identification and analysis of such effects should be straightforward on the basis of the calculations presented in this work.<sup>40</sup>

**Acknowledgment.** This work was supported by the Swedish Medical Research Council (MFR, Grant 0006) and the Swedish Natural Science Research Council (NFR). The calculations were done on the CRAY XMP/416 of the Nationellt Superdatorcentrum (NSC), Linköping, Sweden, and on a Silicon Graphics Power Challenge at the MEDNET Laboratory. The authors thank the NSC for a generous allotment of computer time and the Skandinaviska Enskilda Bankens Foundation for a generous grant for computer equipment.

## References and Notes

- (1) Pascher, I.; Lundmark, M.; Nyholm, P.-G.; Sundell, S. *Biochim. Biophys. Acta* **1992**, *1113*, 339.
- (2) Pullman, B.; Berthod, H. *FEBS Lett.* **1974**, *44*, 266.
- (3) Pullman, B.; Berthod, H.; Gresh, N. *FEBS Lett.* **1975**, *53*, 199.
- (4) Pullman, B.; Saran, A. *Int. J. Quantum Chem., Quantum Biol. Symp.* **1975**, *71*.
- (5) Frischleder, H.; Peinel, G. *Chem. Phys. Lipids* **1982**, *30*, 121.
- (6) Frischleder, H.; Lochmann, R. *Int. J. Quantum Chem.* **1979**, *16*, 203.



- (7) Kreissler, M.; Lemaire, B.; Bothorel, P. *Biochim. Biophys. Acta* **1983**, *735*, 12.
- (8) Hadzi, D.; Hodoscek, M.; Grdadolnik, J.; Avbelj, F. *J. Mol. Struct.* **1992**, *266*, 9.
- (9) Liang, C.; Ewig, C. S.; Stouch, T. R.; Hagler, A. T. *J. Am. Chem. Soc.* **1993**, *115*, 1537.
- (10) Stewart, J. J. P. *J. Comput. Chem.* **1989**, *10*, 209.
- (11) Stewart, J. J. P. *J. Comput. Chem.* **1989**, *10*, 221.
- (12) Stewart, J. J. P. *MOPAC, A Semi-Empirical Molecular Orbital Program*; QCPE: Bloomington, IN, 1983.
- (13) Binkley, J. S.; Pople, J. A.; Hehre, W. J. *J. Am. Chem. Soc.* **1980**, *102*, 939.
- (14) Gordon, M. S.; Binkley, J. S.; Pople, J. A.; Pietro, W. J.; Hehre, W. J. *J. Am. Chem. Soc.* **1982**, *104*, 2797.
- (15) Pietro, W. J.; Francl, M. M.; Hehre, W. J.; Defrees, D. J.; Pople, J. A.; Binkley, J. S. *J. Am. Chem. Soc.* **1982**, *104*, 5039.
- (16) Hehre, W. J.; Ditchfield, R.; Pople, J. A. *J. Chem. Phys.* **1972**, *56*, 2257.
- (17) Hariharan, P. C.; Pople, J. A. *Theor. Chim. Acta* **1973**, *28*, 213.
- (18) Gordon, M. S. *Chem. Phys. Lett.* **1980**, *76*, 163.
- (19) Frisch, M. J.; Pople, J. A.; Binkley, J. S. *J. Chem. Phys.* **1984**, *80*, 3265.
- (20) Chandrasekhar, J.; Andrade, J. G.; Schleyer, P. v. R. *J. Am. Chem. Soc.* **1981**, *103*, 5609.
- (21) (a) Spitznagel, G. W.; Clark, T.; Chandrasekhar, J.; Schleyer, P. v. R. *J. Comput. Chem.* **1982**, *3*, 363. (b) Clark, T.; Chandrasekhar, J.; Spitznagel, G. W.; Schleyer, P. v. R. *J. Comput. Chem.* **1983**, *4*, 294.
- (22) Hehre, W. J.; Radom, L.; Schleyer, P. v. R.; Pople, J. A. *Ab Initio Molecular Orbital Theory*; John Wiley & Sons: New York, 1986.
- (23) Pople, J. A.; Binkley, J. S.; Seeger, R. *Int. J. Quantum. Chem. Symp.* **1976**, *10*, 1.
- (24) Sundaralingam, M. *Ann. N. Y. Acad. Sci.* **1972**, *195*, 324.
- (25) Cremer, D. *J. Chem. Phys.* **1978**, *69*, 4456.
- (26) The  $C_2$  axis is perpendicular to the plotting plane passing through the point  $\alpha_2 = \alpha_3 = 0^\circ$ ; the symmetry planes are also perpendicular to the plotting plane and are defined by the lines  $\alpha_2 = \alpha_3$  and  $\alpha_2 = -\alpha_3$ .
- (27) Hauser, H.; Pascher, I.; Pearson, R. H.; Sundell, S. *Biochim. Biophys. Acta* **1981**, *650*, 21.
- (28) Samra, R.; Ramirez, F.; Narayana, P.; McKeever, B.; Okazaki, H.; Marecek, J. F. *J. Am. Chem. Soc.* **1978**, *100*, 4453.
- (29) Allen, F. H.; Kennard, O.; Taylor, R. *Acc. Chem. Res.* **1983**, *16*, 146.
- (30) Cremer, D.; Pople, J. A. *J. Am. Chem. Soc.* **1975**, *97*, 1358.
- (31) Cremer, D. *J. Chem. Phys.* **1979**, *70*, 1898.
- (32) Cremer, D. *Isr. J. Chem.* **1983**, *23*, 72.
- (33) The correct notation is  $V_{10} + V_{01}$  rather than  $V_{10}$ ,  $V_{20} + V_{02}$  rather than  $V_{20}$ , etc.
- (34) Geometric mean of P-O(C) bond lengths from a search on all types of phosphodiester in the Cambridge structural database.
- (35) Lemieux, R. U. In *Molecular Rearrangements*; De Mayo, P., Ed.; Interscience: New York, 1964; p 723.
- (36) Eliel, E. L. *Angew. Chem.* **1972**, *84*, 779.
- (37) Deslongchamps, P. *Stereoelectronic Effects in Organic Chemistry*; Pergamon: Oxford, U.K., 1983.
- (38) Dewar, M. J. S.; Thiel, W. *J. Am. Chem. Soc.* **1977**, *99*, 4899.
- (39) Dewar, M. J. S.; Zoebisch, E. G.; Healy, E. F.; Stewart, J. J. P. *J. Am. Chem. Soc.* **1985**, *107*, 3902.
- (40) Landin, J.; Cremer, D.; Pascher, I. To be published.

JP942483X